Optical coherent transients induced by time-delayed fluctuating pulses: Three-pulse transients

V. Finkelstein and P. R. Berman
Department of Physics, New York University, 4 Washington Place, New York, New York 10003
(Received 8 January 1990)

A theoretical analysis of the optical coherent transients that arise when a sample of two-level atoms is irradiated by a sequence of three broad-bandwidth pulses is presented. The first two pulses have a relative delay time of order of the correlation time of the pulse fluctuations and are sent into an atomic vapor from different directions. These pulses, whose temporal width is much greater than the delay time, can be correlated with one another and can be strong enough to saturate the two-level atomic transition. The third pulse is weak, noncorrelated with the first two, and is delayed in time so that it does not overlap them. We present a detailed examination of the transient signal that is produced when the third pulse is scattered by the spatial gratings in the population difference of atoms created by the first two pulses. Taking into account the effects of inhomogeneous and homogeneous broadening, we calculate the intensity of the transient signal, emitted in different directions, as a function of delay time. The signal is found to depend dramatically on the intensities of the excitation pulses. It is shown that, for strong excitation pulses, there is a direct dependence of the signal on the cross-correlation time of pulses τ_c^{12} that does not exist when the pulses are weak. In particular, the strongest signals exhibit a peak of width of order τ_c^{12}. This peak can have a very narrow dip near its maximum whose width is much smaller than τ_c^{12}, if the pulses are fully correlated. We develop a representation of the time evolution of the Bloch vector of a two-level atom, driven by time-delayed pulses, that enables us to explain our results. In this representation, the two time-delayed pulses are replaced by two fully overlapping pulses having some effective amplitudes and atomic field detunings.

I. INTRODUCTION

Experiments in which coherent transients are produced by time-delayed, correlated, fluctuating optical pulses[1-18] have received a great deal of attention in the last few years, owing to their potential as a source of subpicosecond time resolution. The advantage of using broad-bandwidth light lies in the fact that under certain conditions, a time resolution may be achieved that is equal to the autocorrelation time τ_c of the applied fields. This autocorrelation time may be orders of magnitude smaller than the pulse duration t_p.

A convenient experimental configuration for observing such optical transients involves sending either two or three laser pulses into an atomic vapor. In this paper we consider only three-pulse transients (PT-3). Two pulses (which may be derived from a single laser), having wave vectors $\mathbf{k}_1$ (pulse 1) and $\mathbf{k}_2$ (pulse 2), respectively, are sent into a sample of two-level atoms [see Fig. 1(a)]. The wave vectors are chosen such that $|\mathbf{k}_1|=|\mathbf{k}_2|=k$ and $\theta=\angle(\mathbf{k}_1,\mathbf{k}_2)\ll 1$. Pulse 2 and pulse 1 have a relative time delay denoted by t_{12}. For $t_{12}>0$ ($t_{12}<0$), pulse 1 precedes (follows) pulse 2 [see Fig. 1(b)]. Under PT-3 conditions these pulses create spatial gratings in the population difference of atoms with Bragg vectors $n\mathbf{k}_d=n(\mathbf{k}_2-\mathbf{k}_1)$, $n=0,\pm 1,\ldots$. These gratings are subsequently probed by a third pulse with a wave vector $\mathbf{k}_3$ that is time delayed by $t_{13}>t_{12}+t_p$ relative to the first excitation pulse. The energy radiated in the directions $\mathbf{k}_3+n\mathbf{k}_d$ is studied

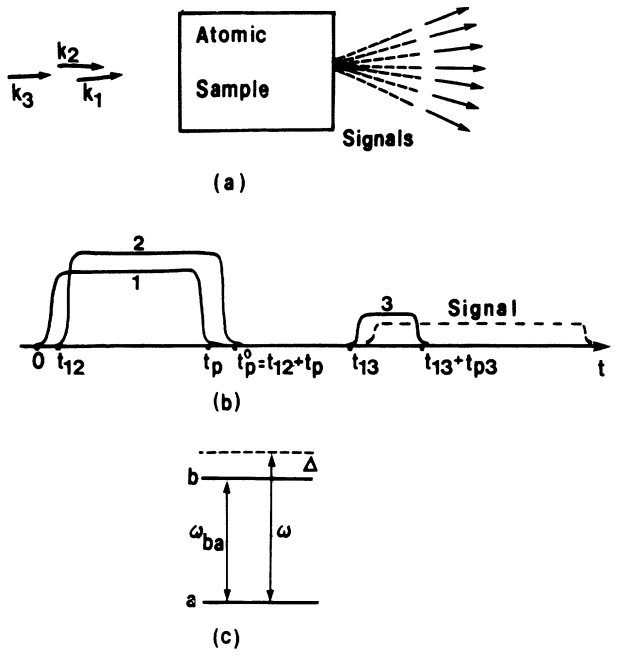

FIG. 1. The three-pulse transient (PT-3) configuration. (a) Angled-beam configuration. (b) The temporal sequence of pulses: for $t_{12}>0$ pulse 1 (wave vector $\mathbf{k}_1$) precedes pulse 2 (wave vector $\mathbf{k}_2$), the third pulse does not overlap the first two pulses. (c) A two-level atom having transition frequency ω_{ba} is driven by the pulses, each having central frequency ω.

as a function of t_{12}.

Although signals can be generated by scattering from nth-order gratings, most experimental work has concentrated on the signals originating from the first-order gratings ($n=\pm 1$). For weak incident pulses or for fully separated pulses, the first-order gratings provide the major contribution to the signal. However, for strong, overlapping incident pulses, higher-order gratings begin to contribute appreciably.

The early experimental results,[1-10] obtained for weak incident fields, have been interpreted in the context of perturbation theory. More recently, however, time-delayed two-pulse[11] and three-pulse transients[12-15] have been examined under conditions in which at least one of the pulses is strong; that is,

$$\alpha t_p \gg 1 ,$$

where $\alpha=f^2\tau_c$, and f is a Rabi frequency associated with a laser field interacting with a two-level atom. The three-pulse experiments are typically carried out at temperatures 300–500 K using excitation pulses having $t_p \approx 10$ ns, and with low buffer gas pressures; consequently, the Doppler width $\Delta_D=ku$ (u is the most probable atomic speed) satisfies the inequalities

$$\Delta_D \gg t_p^{-1}, T_1^{-1}, T_2^{-1} , \tag{1.1}$$

where T_1 and T_2 are longitudinal and transverse relaxation times, respectively.

In the strong-field regime the signal energy as a function of the delay time t_{12} may depend on the correlation time τ_c itself,[14,15] while the dependence of the signal on the Doppler width of the atomic ensemble is minimal. Such behavior differs sharply from that in a weak-field regime when the signal strongly depends on the Doppler width, and the correlation time does not play a separate role in the effects under consideration. Currently the nature of the phenomena observed in a strong-field regime remains unclear.

Theoretical analysis of the experimental results brings into play many profound theoretical problems concerned with studies of the stochastic Bloch equations in the intense field regime. A number of papers have been devoted to this problem in the last twenty-five years[19-40] and numerous effects have been discussed assuming fluctuating radiation fields (resonant fluorescence, double resonance, multiphoton ionization, optical induction decay, Hanle effect, etc.). In most of these calculations, the response of an atomic ensemble to a fluctuating field has been studied as a function of the noise properties of the fields. In many cases the noise was assumed to be Markovian in nature. The problem under consideration herein differs in that atoms are subjected to two time-delayed noise fields which may be correlated. Thus, the atoms retain some memory of the first field when the second field acts. Even if the noise of each field is Markovian, the combined effect of the two fields is non-Markovian, in general, owing to these memory effects. This feature greatly complicates the calculations. Initial attempts at solutions employed diagrammatic methods.[14,41] Later, a decorrelation approximation[42] was used and results were obtained[15] in the limit of stationary atoms subjected to fully correlated, time-delayed fields, one of which was weak, while another was strong: $\alpha_1 t_p \ll 1 \ll \alpha_2 t_p$ [$\alpha_i=|f_i|^2\tau_c$ ($i=1,2$), f_i is Rabi frequency associated with field i]. It was shown theoretically, and has been confirmed experimentally, that under these conditions the radiated energy $W_1^{(3)}(t_{12})$ exhibits a narrow dip centered at $t_{12}=0$, superimposed on a broad background signal. The dip has a width of order τ_c and relative depth equal to 0.5

This observation motivates us to consider the limiting, but important, case in which the correlation and delay times are sufficiently small to satisfy

$$\tau_c, t_{12} \ll \alpha^{-1}, t_p, \Delta_D^{-1}, T_1, T_2 . \tag{1.2}$$

No restriction is imposed on the ratio t_{12}/τ_c. Under these conditions we have found a closed form solution for the signal energy, valid for arbitrary field intensities and relaxation rates. Some direct dependence of the observed signal on τ_c will be shown to exist in the strong-field regime; the interpretation of this effect is given in terms of some additional detuning parameter that appears in the Bloch equations as a result of the time delay of the pulses. The conditions required for observation of the studied phenomena are discussed.

In Sec. II we derive the laser fields and quantum system to be considered, and present the general expressions for the measured energy of the signal in the PT-3 case in terms of a single-time, two-atom correlation function. Using the Bloch vector model, in Sec. III we develop a new representation which permits us to analyze the dynamics of a two-level atom driven by the time-delayed pulses as if the pulses are fully overlapping. The equations for single-time two-atom correlation functions averaged over field fluctuations, which are needed in the calculation, are derived in Sec. IV. In Sec. V we describe a general solution to the problem. A weak-relaxation limit is discussed in Sec. VI. An explanation of the dependence of the signal on time delay t_{12} is presented in Sec. VII and the relative dephasing of the Bloch vectors in a strong-field regime that leads to the results obtained in Sec. VI is considered qualitatively. The results obtained in a strong-relaxation limit are discussed in Sec. VIII.

II. BASIC ASSUMPTIONS AND EQUATIONS

A. Laser field

We consider an ensemble of two-level atoms each having transition frequency ω_{ba} [excited state b, ground state a, as shown in Fig. 1(c)]. Atoms interact with two laser pulses of duration t_p, time delayed relative to each other by an interval t_{12}. These classical incident fields can be represented as

$$\mathcal{E}(\mathbf{r},t)=\frac{e^{-i\omega t}}{2}\{\mathcal{E}_1(t)\exp(i\mathbf{k}_1\cdot\mathbf{r}) + \mathcal{E}_2(t-t_{12})\exp[i(\omega t_{12}+\mathbf{k}_2\cdot\mathbf{r})]\} + \text{c.c.} , \tag{2.1}$$

where, without loss of generalization, we take all fields having parallel polarization. It is assumed that the atom-field detuning, $\Delta=\omega_{ba}-\omega$, satisfies $|\Delta|\ll\omega$, and that $\mathcal{E}_1$ and $\mathcal{E}_2$ are slowly varying complex field amplitudes satisfying

$$|\dot{\mathcal{E}}_1/\mathcal{E}_1|,|\dot{\mathcal{E}}_2/\mathcal{E}_2|\ll\frac{c|\mathbf{k}_1|}{L|\mathbf{k}_d|},\omega ,$$

where c is the speed of light, L is a characteristic length of the sample, and

$$\mathbf{k}_d=\mathbf{k}_2-\mathbf{k}_1 .$$

We introduce the Rabi frequency $f_i=\mu_{ab}\mathcal{E}_i\hbar^{-1}$ $(i=1,2)$ associated with field $\mathcal{E}_i$; μ_{ab} is the dipole moment matrix element of the $a\rightarrow b$ transition. Both of the pulses are characterized by a broad spectrum, and the amplitudes $\mathcal{E}_1$ and $\mathcal{E}_2$ and, consequently, the Rabi frequencies f_1 and f_2 are treated as complex stationary stochastic processes that may be correlated with each other. In particular, we assume that

$$\begin{aligned}&\langle f_1^*(t)f_1(t-\tau)\rangle=\alpha_1 g_{11}(\tau) ,\\&\langle f_2^*(t)f_2(t-\tau)\rangle=\alpha_2 g_{22}(\tau) ,\\&\langle f_1(t)f_1(t-\tau)\rangle=0,\quad\langle f_2(t)f_2(t-\tau)\rangle=0 ,\end{aligned}\tag{2.2}$$

and

$$\begin{aligned}&\langle f_1(t)f_2(t-\tau)\rangle=0,\quad\langle f_1(t)\rangle=\langle f_2(t)\rangle=0 ,\\&\langle f_1^*(t)f_2(t-\tau)\rangle=\alpha_{12}g_{12}(\tau) ,\end{aligned}\tag{2.3}$$

where the average is over all possible realizations of the fluctuating fields. The quantity $g_{ij}(\tau)$ $(i,j=1,2)$ is a correlation function normalized such that

$$\int_0^\infty g_{ij}(\tau)d\tau=1,\quad i,j=1,2$$

and the autocorrelation parameters α_1 and α_2 are given by

$$\alpha_i=\langle|f_i(t)|^2\rangle\tau_c^{ii},\quad i=1,2$$

while the cross-correlation parameter α_{12} that determines the mutual coherence of the Rabi frequencies is equal to

$$\alpha_{12}=\langle f_1^*(t)f_2(t)\rangle\tau_c^{12} .\tag{2.4}$$

Correlation times are defined by

$$\tau_c^{ij}=g_{ij}^{-1}(0) .\tag{2.5}$$

The cross-correlation time τ_c^{12} cannot be larger than autocorrelation times τ_c^{11},τ_c^{22}, and it follows that

$$\Phi=\frac{\alpha_{12}^2}{\alpha_1\alpha_2} ,\tag{2.6}$$

which is a measure of the relative coherence of the pulses, satisfies

$$0\le\Phi\le1 .$$

For fully correlated pulses $\Phi=1$, while for noncorrelated pulses $\Phi=0$.

According to Eqs. (2.2) and (2.3), the statistical properties of the total field (2.1) are characterized not only by the correlation time τ_c^{ij} but also by the delay time t_{12}, provided the correlation parameter $\Phi\neq0$. In this paper the correlation times τ_c^{ij} as well as the delay time t_{12} are assumed to be much smaller than any characteristic time in the problem [see Eq. (1.2)], but can be comparable to each other; that is

$$\tau_c^{ij},t_{12}\ll\Delta_D^{-1},t_p,\alpha_1^{-1},\alpha_2^{-1},\Delta^{-1},T_1,T_2 .\tag{2.7}$$

In the three-pulse transient, the third pulse is assumed to be weak $(\alpha_3 t_p\ll1)$, to have a broad bandwidth $(\tau_c^{33}\sim\tau_c^{ij})$, and to be uncorrelated with the first two pulses. It is switched on after both the first two excitation pulses and any transients associated with them have already died out. Equation (2.7) defines the delay times for which the theory is applicable.

It is also assumed that the transverse Doppler effect is negligible:

$$\frac{|\mathbf{k}_d|}{|\mathbf{k}_1|}\Delta_D t_p\ll1 ,$$

enabling us to set $\mathbf{k}_1,\mathbf{k}_2\approx\frac{1}{2}(\mathbf{k}_1+\mathbf{k}_2)=\mathbf{k}$ in certain expressions.

B. Dynamical equations

In the rotating-wave approximation the following equations then hold for density matrix elements of a two-level atom having velocity $\mathbf{v}$:

$$\begin{aligned}\dot\rho_1&=-\gamma_t\rho_1+\delta\rho_2+Y\rho_3 ,\\\dot\rho_2&=-\delta\rho_1-\gamma_t\rho_2-X\rho_3 ,\\\dot\rho_3&=-Y\rho_1+X\rho_2-\gamma_l(\rho_3-\rho_{3e}) ,\end{aligned}\tag{2.8}$$

where

$$\begin{aligned}&\rho_1=2\,\mathrm{Re}(\rho_{ab}e^{i(\omega t-\mathbf{k}_2\cdot\mathbf{r})}) ,\\&\rho_2=2\,\mathrm{Im}(\rho_{ab}e^{i(\omega t-\mathbf{k}_2\cdot\mathbf{r})}) ,\\&\rho_3=\rho_{aa}-\rho_{bb},\quad\rho_{aa}+\rho_{bb}=1 ,\end{aligned}$$

and

$$\begin{aligned}&X(t)=X_1(t)+X_2(t-t_{12}) ,\\&Y(t)=Y_1(t)+Y_2(t-t_{12}) ,\\&X_1=-\mathrm{Re}[f_1(t)e^{-i\phi}],\quad Y_1=-\mathrm{Im}[f_1(t)e^{-i\phi}] ,\\&X_2=-\mathrm{Re}[f_2(t-t_{12})],\quad Y_2=-\mathrm{Im}[f_2(t-t_{12})] ,\\&\phi=\mathbf{k}_d\cdot\mathbf{r}-\omega t_{12},\quad\delta=\Delta+kv_z ,\\&f_i(t)=\mu_{ab}\mathcal{E}_i(t)\hbar^{-1},\quad i=1,2\end{aligned}\tag{2.9}$$

and ρ_{3e} is the population difference ρ_3 at thermal equilibrium. The transverse relaxation rate $\gamma_t=T_2^{-1}$ can be expressed as the sum of the spontaneous relaxation rate, $\gamma_l=T_1^{-1}$, of level b and a collisional contribution γ_{coll} as

$$\gamma_t=\frac{\gamma_l}{2}+\gamma_{\mathrm{coll}} .$$

All the dependence on position of the atoms is contained in the phase parameter ϕ; the z axis is taken in the $\mathbf{k}_d$ direction.

Equations (2.8) can be represented as

$$\dot{\rho}_m = \sum_k a_{mk}\rho_k + \gamma_l \rho_{3e}\delta_{m3}, \quad m=1,2,3 , \tag{2.10}$$

where

$$\underline{A}=[a_{mk}]=\underline{A}^0-\underline{\Gamma} ,$$
$$\underline{A}^0=[a^0_{mk}]=\begin{bmatrix} 0 & +\delta & Y \\ -\delta & 0 & -X \\ -Y & X & 0 \end{bmatrix} , \tag{2.11}$$
$$\underline{\Gamma}=\begin{bmatrix} \gamma_t & 0 & 0 \\ 0 & \gamma_t & 0 \\ 0 & 0 & \gamma_l \end{bmatrix} .$$

The components (ρ_1,ρ_2,ρ_3) are the standard components of the Bloch vector $\mathbf{R}(t;\phi,\delta)$, which, according to Eqs. (2.8)–(2.10), may be written in series form as

$$\mathbf{R}(t;\phi,\delta)=\sum_{k=-\infty}^{+\infty}\mathbf{R}^{(k)}(t;\delta)\exp(ik\phi) , \tag{2.12}$$

where $\mathbf{R}^{(k)}$ has components $(\rho_1^{(k)},\rho_2^{(k)},\rho_3^{(k)})$ and

$$\mathbf{R}^{(k)}=(\mathbf{R}^{(-k)})^* . \tag{2.13}$$

We often will refer to $\rho_3^{(n)}$ as the nth-order population grating, even though it is a Fourier component corresponding to the nth-order spatial grating.

C. Signal energy

The aim of this paper consists in studying the signal emitted in the direction $\mathbf{k}_3+n\mathbf{k}_d$. In particular, it is the pulse intensity as a function of a delay time which is the subject of investigation. When deriving the general expressions for this quantity, we do not restrict ourselves to any particular shape of the pulse envelopes.

It is shown in Appendix A that, if the third pulse is weak and is not correlated with the first two excitation pulses, the PT-3 signal intensity in the direction $\mathbf{k}_3+n\mathbf{k}_d$ is proportional to the quantity defined by

$$W_n^{(3)}=\frac{\sqrt{2}}{\Delta_D\pi\sqrt{\pi}}\int\int\frac{\psi(\delta-\Delta)\psi(\tilde{\delta}-\Delta)}{2\gamma_t+i\delta_-} \times\langle T_{33}^{(n,-n)}(t_p^0;\delta,\tilde{\delta})\rangle d\delta\, d\tilde{\delta} , \tag{2.14}$$

where

$$\langle T_{33}^{(n,-n)}(t;\delta,\tilde{\delta})\rangle=\langle\rho_3^{(n)}(t;\delta)\rho_3^{(-n)}(t;\tilde{\delta})\rangle \tag{2.15}$$

and

$$\psi(\delta)=\exp\left[-\frac{\delta^2}{\Delta_D^2}\right]$$

is a Maxwellian distribution function, $t_p^0=t_p+t_{12}$ is the time immediately following the two-excitation pulse sequence, and

$$\delta_-=\delta-\tilde{\delta} .$$

We refer to $W_n^{(3)}(t_{12})$ as the PT-3 signal intensity. It is seen from Eq. (2.14) that the signal depends on the average product of Fourier components (2.12) of two Bloch vectors, associated with different atoms. In Eq. (2.14) and all subsequent equations, a tilde denotes variables of a second atom, i.e., $\tilde{\delta}=\Delta+k\bar{v}_z$.

The problem is reduced to obtaining a two-atom signal-time correlation function for the population difference ρ_3. It will be shown that in a strong-field regime, the gratings in the population difference fluctuate considerably; consequently, the correlation function (2.15) cannot be factorized. In order to solve the problem, we have to consider the second moments of the density matrix elements defined by

$$T_{mm'}=\rho_m(t;\phi,\delta)\rho_{m'}(t;\tilde{\phi},\tilde{\delta})=\rho_m\tilde{\rho}_{m'} .$$

It follows from Eqs. (2.10) that components of the matrix $T_{mm'}$ evolve as

$$\dot{T}_{mm'}=\sum_k(a_{mk}T_{km'}+\tilde{a}_{m'k}T_{mk}) +\gamma_l(\rho_m\delta_{m'3}+\tilde{\rho}_{m'}\delta_{m3}) . \tag{2.16}$$

The solution of this equation averaged over field fluctuations gives the function

$$T=\langle T_{33}(t;\phi,\tilde{\phi},\delta,\tilde{\delta})\rangle ,$$

from which one can extract the Fourier component

$$T^{(n,-n)}(t;\delta,\tilde{\delta})=\frac{1}{4\pi^2}\int\int_{-\pi/2}^{3\pi/2}T(t;\phi,\tilde{\phi},\delta,\tilde{\delta}) \times e^{-in(\phi-\tilde{\phi})}d\phi\, d\tilde{\phi} \tag{2.17}$$

needed in Eq. (2.14). It also will prove useful to introduce the change of variables

$$\phi_-=\tfrac{1}{2}(\phi-\tilde{\phi}),\quad \phi_+=\tfrac{1}{2}(\phi+\tilde{\phi}) , \tag{2.18}$$

and rewrite Eq. (2.17) as

$$T^{(n,-n)}(t;\delta,\tilde{\delta})=\frac{1}{2\pi^2}\int_{-\pi/2}^{\pi/2}d\phi_-\int_{-\pi/2}^{3\pi/3}d\phi_+e^{-i2n\phi_-}T(t;\phi_-,\phi_+,\delta,\tilde{\delta}) . \tag{2.19}$$

Hereafter we take ϕ and $\tilde{\phi}$ in the simplified form

$$\phi=\mathbf{k}_d\cdot\mathbf{r},\quad \tilde{\phi}=\mathbf{k}_d\cdot\tilde{\mathbf{r}}$$

instead of using the rigorous definition (2.9), as the term ωt_{12} leads only to a shift of origin of coordinates and does not affect the Fourier component (2.19) and, consequently, the PT-3 signal.

The signal (2.14) can be written as a sum of two terms, one an even function of t_{12} and the other an odd function of t_{12}. Using both Eq. (2.13) and the fact that T is unchanged if α_1 and α_2 are interchanged, one can show that $T^{(n,-n)}\equiv\langle T_{33}^{(n,-n)}\rangle$ can be written as

$$T^{(n,-n)}(t_p^0;\delta,\tilde{\delta})=N_1(\delta_-,\delta_+)+is\delta_-N_2(\delta_-,\delta_+) \tag{2.20}$$

with N_1 and N_2 being real functions which are even with respect to t_{12}, $\delta_-=\delta-\tilde{\delta}$, and $\delta_+=\delta+\tilde{\delta}$. The parameter s is given by

$$s=\begin{cases}1 \text{ if } t_{12}\geq 0\\ -1 \text{ if } t_{12}<0\end{cases}. \tag{2.21}$$

If γ_t is much smaller than any characteristic spectral width in the system, Eq. (2.14) can be simplified by using the following approximation:

$$(2\gamma_t+i\delta_-)^{-1}=\pi\delta(\delta_-)-iP\left[\frac{1}{\delta_-}\right] \tag{2.22}$$

with $\delta(\ )$ being the δ function and P denoting a principal value. Taking into account Eqs. (2.22) and (2.20), we finally obtain from Eq. (2.14)

$$W_n^{(3)}=(\Delta_D\sqrt{2\pi})^{-1}\int_{-\infty}^{\infty}\psi\left[\frac{\delta_+}{\sqrt{2}}-\sqrt{2}\Delta\right]\left[N_1(0,\delta_+)+\frac{2s}{\pi}\int_0^{\infty}\psi\left[\frac{\delta_-}{\sqrt{2}}\right]N_2(\delta_-,\delta_+)d\delta_-\right]d\delta_+ . \tag{2.23}$$

The first term in (2.23), which is an even function of t_{12}, involves a single integral over δ_+ (or, equivalently, over velocity); consequently, this term can be interpreted as arising independently from the different velocity groups of atoms. The second term in (2.23) is responsible for an asymmetry in the signal as a function of the delay time t_{12}; it involves a double integral over velocities.

III. FULLY OVERLAPPING PULSES VERSUS TIME-DELAYED PULSES: WHAT IS THE DIFFERENCE?

If the excitation pulses fully overlap, i.e., $t_{12}=0$, the non-Markovian nature of the problem related to the time delay is removed. As a result, all the standard methods for treating fields with short correlation times can be applied. What may be less obvious, however, is that, owing to conditions (2.7), these methods also work for nonzero delay times. Before going into the details of such a calculation, we introduce a model which enables us to gain some physical insight into the dynamics of two-level atoms interacting with time-delayed pulses. We do not take into account the relaxation processes at this point, as they play no role in the particular phenomena discussed in this section.

For nonzero delay time we would like to represent the position of the Bloch vector at time t_p^0 as a result of some rotation performed under the influence of two pulses which are fully overlapping rather than spaced apart in time as is the actual case. In other words, we replace the two time-delayed pulses by two, modified simultaneous ones. The new pulses produce the same effect as the two time-delayed pulses. This representation will let us formulate the effect of the time delay in a simple and systematic manner.

It is well known that in the absence of relaxation Eqs. (2.8) can be rewritten in a vector form as

$$\dot{\mathbf{R}}=[\mathbf{H}\times\mathbf{R}],\quad \mathbf{H}=\begin{bmatrix}X\\ Y\\ -\delta\end{bmatrix}, \tag{3.1}$$

where X and Y as defined in Eq. (2.9) are the real and imaginary parts, respectively, of the Rabi frequency associated with the electric field amplitude, taken with the negative sign.

Let us consider the rotation of the Bloch vector $\mathbf{R}$ under the influence of two arbitrary time delayed pulses. It is always possible to find a time t_0, such that the Rabi frequency $f(t)$ of any pulse is negligibly small for $t<t_0$. The exact value of t_0 does not play any role, so we put it equal to zero.

According to Eqs. (2.9) the angular velocity $\mathbf{H}$ equals

$$\mathbf{H}=\mathbf{H}_1(t)+\mathbf{H}_2^-(t),$$

where

$$\mathbf{H}_2^-(t)=\mathbf{H}_2(t-t_{12}),$$

$$\mathbf{H}_1=\begin{bmatrix}X_1(t)\\ Y_1(t)\\ -\delta\end{bmatrix},\quad \mathbf{H}_2=\begin{bmatrix}X_2(t)\\ Y_2(t)\\ 0\end{bmatrix}. \tag{3.2}$$

At time $t=2t_{12}$ the position of the Bloch vector $\mathbf{R}(2t_{12})$ results from two consecutive rotations, each of duration t_{12}. During the first one, an atom is driven by the first excitation pulse only. The Bloch vector rotates with angular velocity

$$\mathbf{H}=\mathbf{H}_1(t),\quad 0\leq t\leq t_{12},$$

and, at $t=t_{12}$, takes the form

$$\mathbf{R}(t_{12})=\mathbf{R}(0)+\int_0^{t_{12}}[\mathbf{H}_1(t')\mathbf{R}(t')]dt' . \tag{3.3}$$

The second rotation is performed under the influence of both pulses (see Fig. 2) with angular velocity

$$\mathbf{H}=\mathbf{H}_1(t)+\mathbf{H}_2(t-t_{12}),\quad t_{12}\le t\le 2t_{12} .$$

The position of the Bloch vector at $t=2t_{12}$ is then given by

$$\mathbf{R}(2t_{12})=\mathbf{R}(t_{12})+\int_{t_{12}}^{2t_{12}}\{[\mathbf{H}_1(t')+\mathbf{H}_2(t'-t_{12})]\mathbf{R}(t')\}dt' . \tag{3.4}$$

We would like to represent the same transition from the starting position $\mathbf{R}(0)$ to the final one $\mathbf{R}(2t_{12})$ as a result of a different sequence of rotations. The second rotation is performed under the influence of the *first* pulse only:

$$\mathbf{H}=\mathbf{H}_1(t),\quad \text{for } t_{12}\le t\le 2t_{12} \tag{3.5}$$

while the first rotation is carried out with an angular velocity

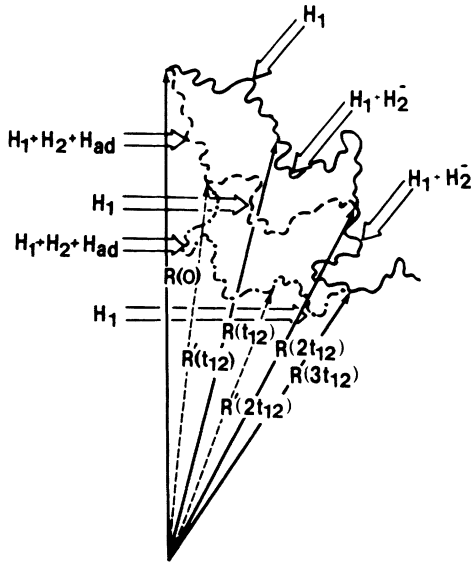

FIG. 2. Schematic representation of stochastic rotation of a Bloch vector $\mathbf{R}$ for given time-delayed fluctuating excitation pulses. Solid curve, the trajectory of the tip of this vector on the surface of a unit sphere. Positions of the Bloch vector at time $t=0,t_{12},2t_{12},3t_{12}$ are represented by solid arrows. Trajectory of the tip of the Bloch vector are shown for $0\le t\le 2t_{12}$ (dashed curve) and $t_{12}\le t\le 3t_{12}$ (dot-dashed curve) using an effective angular velocity corresponding to fully overlapping pulses (see text). Dashed arrows represent the modified intermediate positions $\mathbf{R}'(t_{12})$ and $\mathbf{R}'(2t_{12})$ of the Bloch vector. Note that at the end of each step of the transformation the position of the actual and modified Bloch vectors coincides, even though they differ throughout the intervals. The wide arrows labeled by various values of $\mathbf{H}$ give the angular velocity in each interval.

$$\mathbf{H}=\mathbf{H}_1(t)+\mathbf{H}_2(t)-\mathbf{H}_{\rm ad}(t),\quad \text{for } 0\le t\le t_{12} , \tag{3.6}$$

where an additional angular velocity component is introduced to achieve the same final position of the Bloch vector (see Fig. 2). In terms of the new angular velocities, the modified intermediate position $\mathbf{R}'(t_{12})$ of the Bloch vector is given by

$$\mathbf{R}'(t_{12})=\mathbf{R}(0)+\int_0^{t_{12}}\{[\mathbf{H}_1(t')+\mathbf{H}_2(t')-\mathbf{H}_{\rm ad}(t')]\mathbf{R}(t')\}dt' \tag{3.7}$$

and may not coincide with the true value $\mathbf{R}(t_{12})$. Using Eq. (3.5), one finds that the final position of the Bloch vector at $t=2t_{12}$ is given by

$$\mathbf{R}(2t_{12})=\mathbf{R}'(t_{12})+\int_{t_{12}}^{2t_{12}}[\mathbf{H}_1(t')\mathbf{R}(t')]dt' . \tag{3.8}$$

Since the delay time satisfies condition (2.7) the Bloch vector rotates only slightly in a time period t_{12} and Eqs. (3.3), (3.4), (3.7), and (3.8) can be solved by iteration. Carrying out the iterations to second order gives us two expressions for $\mathbf{R}(2t_{12})$ in terms of $\mathbf{R}(0)$. These expressions are identical provided that

$$\mathbf{H}_{\rm ad}(t)=\int_t^{t+t_{12}}[\mathbf{H}_1(t')\mathbf{H}_2(t)]dt' . \tag{3.9}$$

From the geometrical point of view, the appearance of $\mathbf{H}_{\rm ad}\neq 0$ is simply a consequence of the fact that two successive rotations with different angular velocity vectors $\mathbf{H}_1$ and $\mathbf{H}_2$ do not coincide with that of a single rotation with $\mathbf{H}=\mathbf{H}_1+\mathbf{H}_2$.

We can carry out a similar transformation for the next time period $t_{12}\le t\le 3t_{12}$ and so forth (see Fig. 2). At each step we obtain the same result (3.9) for the time intervals $nt_{12}\le t\le(n+1)t_{12}$, $n=1,2\ldots$. When this transformation is completed up to the time $t=t_p^0$ we get the correct position of the Bloch vector, $\mathbf{R}(t_p^0)$, although all the intermediate values $\mathbf{R}'(nt_{12})$ differ from their true values. The vector $\mathbf{R}(t_p^0)$ can be regarded now as a result of the rotation performed under the influence of the two fully overlapping modified pulses along with some modified atom-field detuning. The modification of the field components and the detuning is given by Eq. (3.9).

If the laser field is fluctuating, the vector $\mathbf{H}_{\rm ad}$ is also a fluctuating function of time. It turns out that the fluctuating part of $\mathbf{H}_{\rm ad}(t)$ results in contributions which are negligible in the limits discussed in this paper. Consequently, the signal depends only on $\langle\mathbf{H}_{\rm ad}\rangle$. Taking into account definitions (2.9) one finds that the only nonzero component of the averaged vector $\langle\mathbf{H}_{\rm ad}\rangle$ lies along the 3 axis and thus describes some additional detuning. This component $h_{{\rm ad},3}$, is given by

$$h_{{\rm ad},3}=\langle\mathbf{H}_{\rm ad}\rangle_3=G(t_{12})\alpha_{12}\sin\phi , \tag{3.10}$$

where

$$G(t_{12})=\int_0^{t_{12}}g_{12}(\tau)d\tau;\quad G(\pm\infty)=\pm 1 . \tag{3.11}$$

The additional detuning $h_{{\rm ad},3}$ is nonzero only for time-delayed pulses ($t_{12}\neq 0$), if both $\alpha_{12}\neq 0$ (the pulses are correlated) and $\phi=\mathbf{k}_d\cdot\mathbf{r}\neq 0$. It depends strongly on the

position $\mathbf{r}$ of the atom and on the delay time t_{12} through the functions ϕ and $G(t_{12})$, respectively. Owing to its dependence on $G(t_{12})$, the absolute value of this additional detuning rises from 0 to $\alpha_{12}|\sin\phi|$ as $|t_{12}|$ varies from 0 to $|t_{12}|>\tau_c^{12}$. Hence, if this additional detuning significantly modifies the dynamics of the two-level atom, we can also expect the PT-3 signal to depend on t_{12} even if $T_{12}\sim\tau_c^{12}$. The implications of this model are explored below.

IV. AVERAGED EQUATIONS FOR THE CORRELATION FUNCTIONS

The single-time two-atom correlation functions $\langle T_{nm}(t)\rangle$ are the solutions of Eqs. (2.16) averaged over histories of the laser fields. A solution for $\langle T_{nm}\rangle$ for the general case of arbitrary t_{12} will be discussed elsewhere.

In this paper we obtain exact results for delay times t_{12} satisfying Eq. (2.7), i.e., sufficiently small that the Bloch vector $\mathbf{R}$, as well as the tensor T_{nm}, varies only slightly during this time period. Nevertheless, it will be shown that the signal (2.14) can vary significantly as a function of t_{12} even under this restriction.

Owing to condition (2.7) we can use the decorrelation approximation[42] when deriving equations for $\langle T_{nm}\rangle$. We follow the method described in Refs. 15 and applied there to this particular problem, extending the method to include effects of relaxation and atomic motion. We obtain the following differential equations for $\langle T_{lm}\rangle$ and $\langle\rho_l\rangle$ that hold true for pulses of arbitrary shape:

$$\langle\rho_1\rangle=\langle\rho_2\rangle=0\ ,$$

$$\dot\rho=-2\alpha(\phi)\rho+\gamma_l(\rho_{3e}-\rho)\ , \tag{4.1}$$

$$\dot T=-2(x+\gamma_l)T+Q(\phi,\tilde\phi)Z+Q^*(\phi,\tilde\phi)Z^*+\gamma_l\rho_{3e}(\rho+\tilde\rho)\ , \tag{4.2}$$

$$\dot Z=-(x+2\gamma_t+i\delta_f)Z+4Q^*T\ , \tag{4.3}$$

where

$$\begin{aligned}&\rho=\langle\rho_3(\delta,\phi)\rangle,\quad\tilde\rho=\langle\rho_3(\tilde\delta,\tilde\phi)\rangle\ ,\\&T=\langle\rho_3(\delta,\phi)\rho_3(\tilde\delta,\tilde\phi)\rangle=\langle\rho_3\tilde\rho_3\rangle=\langle T_{33}\rangle\ ,\\&Z=\langle(\rho_1+i\rho_2)(\tilde\rho_1-i\tilde\rho_2)\rangle\\&\quad=\langle T_{11}+T_{22}+i(T_{21}-T_{12})\rangle\ ,\end{aligned} \tag{4.4}$$

and

$$\alpha(\phi)=\tfrac{1}{2}(\alpha_1+\alpha_2+2\alpha_{12}\cos\phi)\ , \tag{4.5}$$

$$\begin{aligned}&x=\alpha(\phi)+\alpha(\tilde\phi)=\alpha_1+\alpha_2+\alpha_{12}(\cos\phi+\cos\tilde\phi)\ ,\\&Q=\tfrac{1}{2}[\alpha_2+\alpha_1e^{i(\phi-\tilde\phi)}+\alpha_{12}(e^{i\phi}+e^{-i\tilde\phi})]\ ,\end{aligned} \tag{4.6}$$

$$\begin{aligned}\delta_f&=[\delta+G(t_{12})\alpha_{12}\sin\phi]-[\tilde\delta+G(t_{12})\alpha_{12}\sin\tilde\phi]\\&=\delta_-+G(t_{12})\alpha_{12}(\sin\phi-\sin\tilde\phi)\ .\end{aligned} \tag{4.7}$$

The function $G(t_{12})$ is given by Eqs. (3.11).

Equations (4.1)–(4.3) describe the first- and second-order density-matrix correlation functions of two atoms located at points $\mathbf{r}$ and $\tilde{\mathbf{r}}$, respectively. We present only three of the nine equations for T_{lm} because, under the approximation applied here, the rest of the equations are decoupled from Eqs. (4.2) and (4.3) and do not play any role in this problem. We shall discuss solutions of Eqs. (4.1)–(4.3) in Sec. V. Before doing so, let us consider the coefficients appearing in these equations. The parameter $2\alpha(\phi)$ which appears in Eq. (4.1) is proportional to the mean intensity of interference fringes at the location of the atom. This parameter is responsible for the decay of $\rho=\langle\rho_3\rangle=\langle\rho_{aa}-\rho_{bb}\rangle$; in other words, $(2\alpha)^{-1}$ is a relaxation parameter whose origin can be traced to the combined action of the fluctuating excitation pulses. In Eqs. (4.2) and (4.3) the parameter x, equal to the sum $\alpha(\phi)+\alpha(\tilde\phi)$ ($\phi=\mathbf{k}_d\cdot\mathbf{r},\tilde\phi=\mathbf{k}_d\cdot\tilde{\mathbf{r}}$), leads to the decay of the averaged, single-time, two-atom correlation function T. Another parameter, Q, proportional to the correlation between interference fringes at different points $\mathbf{r}$ and $\tilde{\mathbf{r}}$, provides coupling between the population correlation function T and the coherence correlation function Z. As $\alpha(\phi)$, x, and Q depend on the cross-correlation parameter α_{12}, we expect the solution of Eqs. (4.1)–(4.3) to differ substantially for correlated ($\alpha_{12}\neq0$) and uncorrelated ($\alpha_{12}=0$) pulses. Finally, we note that quantity δ_f defined as a difference of modified detunings in Eq. (4.7), appears in Eq. (4.3). In Eq. (4.7), one sees that the atom-field detuning δ is altered by a term $G(t_{12})\alpha_{12}\sin\phi$ [see Eq. (3.10)], whose origin was explained in the previous section and which is the only parameter in Eqs. (4.1)–(4.3) that depends on the delay time t_{12}.

V. RECTANGULAR PULSES

In this paper we consider pulses with rectangular envelopes

$$f(t)=\text{const}\neq0\quad\text{for } 0\le t\le t_p\ ,$$

for which the coefficients (4.5) in Eqs. (4.1)–(4.3) do not vary with time. Although the assumption of rectangular pulses may seen to be a severe restriction, it turns out that many of the results obtained are independent of pulse shape.

The ensemble of two-level atoms is assumed to be in thermal equilibrium before the excitation pulses are applied at $t=0$. The corresponding initial conditions are

$$\begin{aligned}&\rho_3(0)=\rho_{aa}(0)-\rho_{bb}(0)=\rho_{3e}\ ,\\&\rho_1(0)=2\,\mathrm{Re}[\rho_{ab}(0)e^{-i\mathbf{k}_2\cdot\mathbf{r}}]=0\ ,\\&\rho_2(0)=2\,\mathrm{Im}[\rho_{ab}(0)e^{-i\mathbf{k}_2\cdot\mathbf{r}}]=0\ ,\end{aligned} \tag{5.1}$$

implying that

$$\rho(0)=\rho_{3e},\quad\langle T(0)\rangle=\rho_{3e}^2,\quad Z(0)=0\ . \tag{5.2}$$

From Eq. (4.1) we find an averaged population difference

$$\rho=\frac{\rho_{3e}}{2\alpha(\phi)+\gamma_l}(\gamma_l+2\alpha e^{-[2\alpha(\phi)+\gamma_l]t}) . \tag{5.3}$$

The solution for the averaged second moment of the population difference can be represented in a general form as

$$T=T_0+\sum_{i=1}^{3} e^{\lambda_i t}T_i+e^{-\gamma_l t}(T_4e^{-2\alpha t}+T_5e^{-2\tilde{\alpha}t}) , \tag{5.4}$$

where T_0 is the steady-state solution

$$T_0=\frac{\gamma_l^2\rho_{3e}^2(x+\gamma_l)[(x+2\gamma_t)^2+\delta_f^2]}{(2\alpha+\gamma_l)(2\tilde{\alpha}+\gamma_l)\{[(x+2\gamma_t)^2+\delta_f^2](x+\gamma_l)-4|Q|^2(x+2\gamma_t)\}} . \tag{5.5}$$

The exponents $\lambda_{1,2,3}$ are the roots of the equation

$$(\lambda+2\gamma_t)(\lambda+2\gamma_t+x)(\lambda+2\gamma_t+3x)=-2y(\lambda+2\gamma_t+x)-\delta_f^2(\lambda+2\gamma_l+2x)-2(\gamma_l-\gamma_t)(\lambda+2\gamma_t+x)^2 \tag{5.6}$$

with

$$y=x^2-4|Q|^2$$
$$=2\alpha_1\alpha_2[1-\cos(\phi-\tilde{\phi})]=\alpha_{12}^2(\sin\phi-\sin\tilde{\phi})^2 . \tag{5.7}$$

The functions T_i $(i=1,2,3)$ are solutions of the homogeneous equations (4.2) and (4.3) ($\rho_{3e}=0$); they correspond to the roots λ_i and take into account the initial conditions (5.2). The exact expressions for $T_{1,2,3}$ are too complicated to be presented here. Limiting values for T_1,T_2,T_3 are given in Sec. VI and Appendix C.

Finally, $T_4(\alpha,\tilde{\alpha})=T_5(\tilde{\alpha},\alpha)$ is given by

$$T_4=\frac{2\gamma_l\rho_{3e}^2\alpha(z^2+\delta_f^2)}{(2\alpha+\gamma_l)[(z^2+\delta_f^2)(2\tilde{\alpha}+\gamma_l)-8|Q|^2z]} , \tag{5.8}$$

where $z=\tilde{\alpha}-\alpha-\gamma_l+2\gamma_t$.

In principle, a numerical integration (2.19) of the general solution (5.4) over ϕ and $\tilde{\phi}$ gives us the desired PT-3 signal. However, to understand the dependence of this signal on the numerous parameters involved, it is useful to obtain some analytical results. They can be obtained for large or small values of a parameter n_0 which characterizes the number of population gratings of comparable amplitude which are generated in the sample, each grating of order n contributing to the signal in direction $\mathbf{k}_3\pm n\mathbf{k}_d$. For $n_0\ll 1$, only the gratings of the first order, $n=\pm 1$, are important. For $n_0\gg 1$, it is possible to integrate (2.19) by noting that regions where $\cos\phi\approx\cos\tilde{\phi}$ give maximum contributions to the PT-3 signal.

Hereafter, we replace $t_p^0=t_p+t_{12}$ by t_p, since under conditions (2.7) the difference between them does not affect the results. We assume that at thermal equilibrium a two-level atom is in its ground state and thus

$$\rho_{3e}=1 . \tag{5.9}$$

Deviation from condition (5.9) leads only to decrease of the PT-3 signal by the factor ρ_{3e}^2. In addition, we drop the $(\phi,\tilde{\phi},\delta,\tilde{\delta})$ arguments and write $T(t;\phi,\tilde{\phi},\delta,\tilde{\delta})$ simply as $T(t)$.

VI. QUANTITATIVE RESULTS IN THE WEAK-RELAXATION LIMIT $\gamma_l T_P\ll 1;\gamma_T T_p\ll 1$

In this section we assume that

$$\gamma_l,\gamma_t\ll t_p^{-1} \tag{6.1}$$

and consequently, the role of relaxation in the formation of the PT-3 signal is negligible, and the signal can be calculated using Eq. (2.23). Most experiments have been carried out in this "weak-relaxation" limit.

A. Weak-field regime

The weak-field regime is defined by

$$\alpha_1,\alpha_2\ll t_p^{-1} . \tag{6.2}$$

In this limit, the population gratings of order $n=\pm 1$ lead to the strongest PT-3 signals. The signals, originating from the $n=1$ and $n=-1$ gratings, are of equal intensity. In the weak-field regime, one can interpret the signals in terms of a four-wave mixing process involving one interaction with each of the three excitation pulses. If inequalities (6.1) and (6.2) hold, one finds (see Appendix B)

$$T^{(1,-1)}(t_p;\delta,\tilde{\delta})=\alpha_{12}^2t_p^2+2\alpha_1\alpha_2\frac{1-\cos(\delta_-t_p)}{\delta_-^2} . \tag{6.3}$$

As $T^{(1,-1)}$ given by (6.3) is a real even function of δ_-, it follows that $N_2=0$ in Eq. (2.20). Hence, to obtain the PT-3 signal from Eq. (2.23), one needs only the expression (6.3) with equal detunings, that is $T^{(1,-1)}(t_p;\delta,\delta)=N_1(\delta_-=0)$, given by

$$T^{(1,-1)}(t_p;\delta,\delta)=t_p^2(\alpha_{12}^2+\alpha_1\alpha_2) . \tag{6.4}$$

To interpret (6.4), one can use Eqs. (2.15) and (2.13) to rewrite $T^{(1,-1)}(t_p;\delta,\delta)$ as

$$T^{(1,-1)}(t_p;\delta,\delta)=\langle|\rho_3^{(1)}(t_p;\delta)|^2\rangle$$
$$=[\rho^{(1)}(t_p)]^2+\langle|\rho_3^{(1)}(t_p;\delta)-\rho^{(1)}(t_p)|^2\rangle , \tag{6.5}$$

where $\rho^{(1)}(t_p)$ is the *mean* amplitude of the population

difference grating, $\rho^{(1)}(t_p)=\langle\rho_3^{(1)}(t_p;\delta)\rangle$. From Eqs. (2.12) and (5.3), and under condition (6.2), one finds that $\rho^{(1)}(t_p)$ is given by

$$\rho^{(1)}(t_p)=\alpha_{12}t_p \ . \tag{6.6}$$

The correlation function (6.4) consists of the two parts. The first term $\alpha_{12}^2t_p^2$ depends on the mutual correlation of the pulses and is equal to the first term in Eq. (6.5), that is, to the square of the mean amplitude $\rho^{(1)}(t_p)$ of the population difference grating. The second term of expression (6.4) equals the average of the square of the fluctuating part of the population difference grating and is independent of the mutual correlation of the pulses. For fully correlated pulses these two contributions are equal.

From Eqs. (2.23) and (6.5) one obtains the PT-3 signal

$$W_1^{(3)}=t_p^2(\alpha_{12}^2+\alpha_1\alpha_2) \tag{6.7}$$

which does not depend on the delay time t_{12}. One might have anticipated this result since, in a weak-field regime, the significant asymmetry of the signal occurs only for long delay times $|t_{12}|\geq\Delta_D^{-1}$,[3,8] for which the Bloch vector can acquire a non-negligible Doppler phase (of order $\Delta_D t_{12}>1$). For t_{12} satisfying inequality (2.7), however, this asymmetry is negligible. For fully correlated pulses ($\Phi=1$), Eq. (6.7) coincides with a previously obtained result.[12]

The important feature of the weak-field result is the absence of a direct dependence of the signals on the correlation time. This dependence emerges only in third order of the parameter αt_p and can be neglected.

One can also see from Eq. (6.7) and the definition of α_{12} that the part of the signal proportional to α_{12}^2, which depends on the correlation of the pulses, cannot be larger than the part proportional to $\alpha_1\alpha_2$, which is independent of this correlation. In a strong field, these properties of the signals are changed dramatically.

B. Strong-field regime

The main objective of this work is to study the regime when at least one of the excitation pulses is strong. In the weak-relaxation limit (6.1), the strong-field criterion is

$$\alpha_{\max}=\max(\alpha_1,\alpha_2)\gg t_p^{-1} \ . \tag{6.8}$$

The PT-3 signal is determined from Eq. (2.17) [which gives $T^{(n,-n)}(t_p)$ in terms of the averaged correlation function $T(t_p)$], Eq. (2.20) [which represents $T^{(n,-n)}(t_p)$ in terms of N_1 and N_2], and Eq. (2.23) (which gives the PT-3 signal as an integral of N_1 over δ_+ and N_2 over $\delta_\pm$). It is shown in Appendix C that $T(t_p)$ is approximately given by

$$T(t_p)=\tfrac{1}{3}e^{\lambda_1 t_p} \ , \tag{6.9}$$

where

$$\lambda_1=-\tfrac{2}{3}\{2\alpha_1\alpha_2[1-\cos(\phi-\tilde{\phi})]$$
$$-[1-G^2(t_{12})]\alpha_{12}^2(\sin\phi-\sin\tilde{\phi})^2+\delta_-^2$$
$$+2\delta_- G(t_{12})\alpha_{12}(\sin\phi-\sin\tilde{\phi})\}$$
$$\times[\alpha_1+\alpha_2+\alpha_{12}(\cos\phi+\cos\tilde{\phi})]^{-1} \ . \tag{6.10}$$

All the other terms in the general expression (5.4) provide corrections to the PT-3 signal which are at most of order $(\alpha_{\max}t_p)^{-1}\ll 1$.

An important feature of the strong-field signal is tied to the two terms in Eq. (6.10) that contain the function $G(t_{12})$. For correlated pulses ($\alpha_{12}\neq 0$; i.e., $\Phi\neq 0$), these terms lead to the variation of the signal on a time scale of τ_c^{12}, since $G(t_{12})$ has been shown to vary over such a time scale. As noted above, Eq. (2.23) is a valid starting point for an analysis of the PT-3 signal in the weak-relaxation limit. The part of the signal which is asymmetrical about $t_{12}=0$ arises from the N_2 term in Eq. (2.23). Both of the terms in Eq. (6.10) depending on $G(t_{12})$ affect this part of the PT-3 signal. It can be shown, however (see Appendix D), that in a strong-field regime the strongest PT-3 signals are characterized by small orders n and are almost symmetrical for $|t_{12}|\leq\alpha^{-1}$. Although the asymmetrical contribution to the signal is usually small, there are certain cases (to be discussed) where it cannot be neglected. If we do not consider this small asymmetry, then according to Eq. (2.23) the PT-3 signal is determined by its symmetrical part, N_1, that depends only on λ_1 ($\delta_-=0$) from Eq. (6.10). Consequently, N_1 is affected only by the term in Eq. (6.15) which is proportional to the parameter $[1-G^2(t_{12})]\alpha_{12}^2$ that varies from α_{12}^2 to 0 as t_{12} varies from 0 to values $\geq\tau_c^{12}$. Thus, for $t_{12}>\tau_c^{12}$ this factor vanishes. Consequently, the numerator of Eq. (6.10) becomes independent of Φ once $t_{12}>\tau_c^{12}$. There is an additional dependence on α_{12} contained in the denominator of Eq. (6.10); however, it turns out this dependence does not significantly modify the signal for small order n. As a result, the signal is nearly independent of Φ for $t_{12}>\tau_c^{12}$; in other words, both correlated or uncorrelated pulses, characterized by $\Phi=1$ and $\Phi=0$, respectively, give rise to almost equal signals for $t_{12}>\tau_c^{12}$.

The detailed calculations of the PT-3 signal are carried out in Appendix D. Below we present the results in the most important cases.

1. *One strong and one weak pulse*

As α_1 and α_2 enter Eq. (6.10) in a symmetric way, the PT-3 signal does not depend on which pulse is strong, and this case is characterized by

$$\alpha_{\max}\gg t_p^{-1}\gg\alpha_{\min} \ , \tag{6.11}$$

where $\alpha_{\min}=\min(\alpha_1,\alpha_2)$. Taking into account Eqs. (6.11) and expanding expression (6.10) to first order in $\alpha_{\min}t_p$, we get the correlation function

$$T(t_p)=\frac{1}{3}\exp\left[-\frac{2\delta_-^2 t_p}{3\alpha_{\max}}\right]\left\{1+\frac{2\alpha_{\min}t_p}{3}\left[[\cos(\phi-\tilde{\phi})-1]\{2-(1-G^2)\Phi[1+\cos(\phi+\tilde{\phi})]\}\right.\right.$$
$$\left.\left.-\frac{2G\Phi\delta_-}{\alpha_{12}}\left[1-\frac{\alpha_{12}}{\alpha_{\max}}(\cos\phi+\cos\tilde{\phi})\right](\sin\phi-\sin\tilde{\phi})\right]\right\}. \tag{6.12}$$

The strongest signals ($n\neq 0$) are emitted in the directions $k_3\pm k_d$. Picking up the terms proportional to $\exp\{i(\phi-\tilde{\phi})\}$ needed in Eq. (2.19) one finds

$$T^{(1,-1)}(t_p)=\frac{\alpha_{\min}t_p}{9}\exp\left[-\frac{2\delta_-^2 t_p}{3\alpha_{\max}}\right]$$
$$\times\left[2-[1-G^2(t_{12})]\Phi-i\frac{2\Phi G\delta_-}{\alpha_{\max}}\right]. \tag{6.13}$$

The signal obtained from Eqs. (2.20) and (2.23) is given by

$$W_1^{(3)}=\frac{\alpha_{\min}t_p}{9}\left[2-[1-G^2(t_{12})]\Phi\right.$$
$$\left.-\frac{2\Phi G}{\sqrt{\pi}}\left[\frac{\alpha_{\max}^2}{2\Delta_D^2}+\frac{2}{3}\alpha_{\max}t_p\right]^{-1/2}\right]. \tag{6.14}$$

Thus, when one of the fields is weak, the PT-3 transient consists of a background signal and a narrow dip of width τ_c^{12} and relative depth $\Phi/2$ centered at zero delay time, $t_{12}=0$ (see Fig. 3). The dip is produced only for correlated pulses ($\Phi\neq 0$) while the background signal exists for either noncorrelated or correlated pulses. The result (6.14) coincides with that obtained earlier[15] for fully correlated pulses, when $\Phi=\alpha_{12}^2(\alpha_1\alpha_2)^{-1}=1$, and for $\alpha_{\max}t_p=\infty$. Owing to condition (6.11), the signal (6.14) is almost symmetrical around $t_{12}=0$ for any Doppler width Δ_D; however, there is a small negative asymmetry which arises from the last term in Eq. (6.14) [the signal at $t_{12}<0$ is larger than at $t_{12}>0$]. Such an asymmetry cannot appear in a weak-field regime.

2. *Both pulses are strong*

This case is described by the condition

$$\alpha_{\min}=\min(\alpha_1,\alpha_2)\gg t_p^{-1}. \tag{6.15}$$

Population gratings of order $n\leq n_0$, with $n_0\gg 1$, are created by these strong fields; consequently, the signal intensity in many directions, $\mathbf{k}_3\pm n\mathbf{k}_d$ with $n\leq n_0$, can be comparable. We need consider only $n\geq 0$, since the signals in the $\mathbf{k}_3-n\mathbf{k}_d$ directions are related to those at $\mathbf{k}_3+n\mathbf{k}_d$ by

$$W_n^{(3)}(t_{12})=W_{-n}^{(3)}(-t_{12}). \tag{6.16}$$

It is possible to obtain analytical expressions for the signal in some important limiting cases provided

$$n\ll\alpha_{\min}t_p. \tag{6.17}$$

If mutual correlation of the pulses is moderate or weak, that is, if

$$\Phi\leq 0.5, \tag{6.18}$$

the PT-3 signal takes the form (see Appendix D)

$$W_n^{(3)}=\frac{e^{-n^2/2\eta^2}}{3\eta\sqrt{2\pi}}\left\{1+\frac{\Phi}{4}\left[[1-G^2(t_{12})]\left[1-\frac{n^2}{\eta^2}\right]-\frac{\beta^2}{4}\left[1+\frac{2n^2}{\eta^2}-\frac{n^4}{\eta^4}\right]+\frac{2Gn\beta}{\eta\sqrt{2\pi(D+1)}}\left[\frac{2+D}{1+D}-\frac{n^2}{\eta^2}\right]\right]\right\}, \tag{6.19}$$

where

$$\eta=\left[\frac{4\alpha_1\alpha_2 t_p}{3(\alpha_1+\alpha_2)}\right]^{1/2},$$
$$\beta=\frac{2(\alpha_1\alpha_2)^{1/2}}{\alpha_1+\alpha_2}, \tag{6.20}$$

and

$$D=\frac{3(\alpha_1+\alpha_2)}{4\Delta_D^2 t_p},$$

and all the terms in parentheses that are proportional to Φ are assumed to be small compared to 1. Note that $D\ll 1$ corresponds to a relatively large Doppler width, and $D\gg 1$ to a relatively small Doppler width.

In the limit that $\Phi=0$ (noncorrelated pulses) the signal (6.19) reduces to

$$W_n^{(3)}(\Phi=0)=\frac{e^{-n^2/2n^2}}{3\eta\sqrt{2\pi}}. \tag{6.21}$$

The signal (6.21) does not depend on t_{12}, and Eq. (6.21) is valid for all $n\ll\eta^2$ [see Eqs. (6.17) and (6.20)].

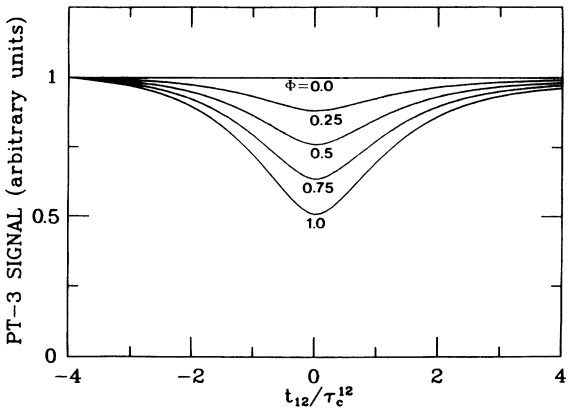

FIG. 3. Signals corresponding to order $n=1$ vs t_{12}/τ_c^{12} in a weak-relaxation limit ($\gamma_l t_p=0.02$ and $\gamma_t t_p=0.01$ in this figure and Figs. 4–10) in the case of one strong and one weak pulse $\alpha_{\max}t_p=300$, $\alpha_{\min}t_p=0.05$, for different degrees of mutual correlation Φ of the pulses; $\Delta_D t_p=14$. All curves in this and all other figures represent numerical solutions of Eqs. (4.1)–(4.3).

The signal (6.19) for correlated pulses differs only slightly from that for uncorrelated pulses, but the difference between the two is a function of t_{12}. The PT-3 signal (6.19) in a direction characterized by $n \ll \eta$ exhibits a small peak having width τ_c^{12} and relative height

$$S=\frac{W_n^{(3)}(t_{12}=t_{12}^{\max})-W_n^{(3)}(t_{12}\gg\tau_c)}{W_n^{(3)}(t_{12}\gg\tau_c)}=\tfrac{1}{4}\Phi\ll 1 \qquad (6.22)$$

(see Fig. 4). The signal has positive asymmetry which is small for any Doppler width and ratio of the pulse intensities. Owing to this asymmetry the central peak maximum of the signal is slightly shifted to positive delay time, that is

$$t_{12}^{\max}=\frac{n\beta}{\eta}\frac{(2+D)}{(1+D)^{3/2}}\tau_c^{12}\ll\tau_c^{12}\ . \qquad (6.23)$$

It is also seen in Eq. (6.19) that the background signal for $t_{12}>\tau_c$ does not exactly equal that for noncorrelated pulses. This difference reaches its maximum value $-\Phi/16\ll 1$ when the pulses have equal intensities, $\alpha_1=\alpha_2$, and the background signal decreases with increasing Φ.

In contrast to the signals corresponding to small n, the signal in a direction characterized by $n\gg\eta$ exhibits a dip (see curve a in Fig. 5), if

$$\frac{n\beta}{\eta\sqrt{1+D}}\ll 1\ . \qquad (6.24)$$

Condition (6.24) can be satisfied if the Doppler distribution is narrow, $D\gg 1$, or the pulses have very different intensities, $\beta\ll 1$ [or $\alpha_{\max}/\alpha_{\min}>10$, see expression (6.20)]. The signal has a small negative asymmetry; the dip is positioned at $t_{12}\approx 0$ and has relative depth

$$|S|=\frac{W_n^{(3)}(t_{12}\gg\tau_c)-W_n^{(3)}(t_{12}=0)}{W_n^{(3)}(t_{12}\gg\tau_c)}=\tfrac{1}{4}\Phi\frac{n^2}{\eta^2}\ll 1\ . \qquad (6.25)$$

However, as soon as condition (6.24) is violated, the dip vanishes and the signal continuously decreases as t_{12} varies from negative to positive values (see curve c in Fig. 5).

If the pulses are strongly correlated, that is if

$$(1-\Phi)\ll 1\ , \qquad (6.26)$$

the qualitative behavior of the PT-3 signal is similar to that considered above; however, all the features are more clearly defined as we proceed to discuss.

First, we consider the strongest signal, characterized by small n, $n\ll\eta$. The intensity of the signal is given by

$$W_n^{(3)}(t_{12})=W_S+W_{AS}\ , \qquad (6.27)$$

where W_S and W_{AS} are correspondingly the symmetrical and asymmetrical parts of the signal

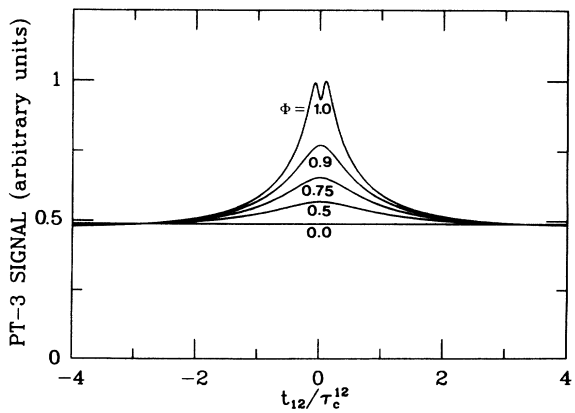

FIG. 4. Signals corresponding to small order $n=1\ll\eta$ vs t_{12}/τ_c^{12} in a weak-relaxation limit in the case when both pulses are strong: $\alpha_{\max}t_p=10^3$, $\alpha_{\min}t_p=10^2$ for different degrees of mutual correlation Φ of the pulses; $\Delta_D t_p=14$.

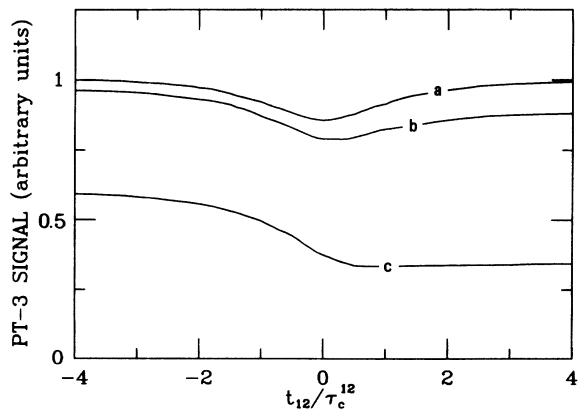

FIG. 5. Signals corresponding to high order $n=20>\eta$ vs t_{12}/τ_c^{12} in a weak-relaxation limit in the case when both pulses are strong: $\alpha_{\min}t_p=100$ and $\alpha_{\max}t_p=10^4$ (curve a), 10^3 (curve b), and 110 (curve c). Degree of mutual correlation of the pulses is moderate: $\Phi=0.25$; $\Delta_D t_p=14$.

$$W_S(t_{12})=W_S(-t_{12});\ W_{AS}(t_{12})=-W_{AS}(-t_{12})\ . \quad (6.28)$$

For $n \ll \eta$, W_S is much larger than W_{AS}, and for $t_{12} \leq \tau_c^{12}$ it can be represented in the form (see Appendix D)

$$W_S=\frac{1}{3\pi\sqrt{2\pi}}\left[W_+ + W_- + \frac{\beta^2}{4\eta}\right], \quad (6.29)$$

with

$$W_\pm=\frac{1}{\eta_\pm}\ln\frac{4\eta_\pm}{n\{\exp(-Z_\pm/2)+[Z_\pm+\exp(-Z_\pm)]^{1/2}\}}, \quad (6.30)$$

and

$$\eta_\pm=\left[\frac{4\alpha_1\alpha_2 t_p}{3(\alpha_1+\alpha_2\pm 2\alpha_{12})}\right]^{1/2}\gg 1\ ,$$
$$Z_\pm=\frac{[1-\Phi(1-G^2)]\eta_\pm^2}{n^2}\ . \quad (6.31)$$

If the pulses are strongly correlated, that is, if $(1-\Phi)<n^2/\eta_\pm^2$, and if the delay time is very small,

$$t_{12}\ll\tau_c^{12}\left[\frac{n^2}{\eta_\pm^2}-(1-\Phi)\right]^{1/2}, \quad (6.32)$$

then $Z_\pm \ll 1$ in Eq. (6.30), and $W_\pm$ increases with increasing t_{12} as

$$W_\pm=\frac{1}{\eta_\pm}\left[\ln\frac{2\eta_\pm}{n}+\frac{[1-\Phi+(t_{12}/\tau_c^{12})^2]\eta_\pm^2}{2n^2}\right]. \quad (6.33)$$

However, when

$$\tau_c^{12}\geq t_{12}>\tau_c^{12}\left[\frac{n^2}{\eta_\pm^2}-(1-\Phi)\right]^{1/2}, \quad (6.34)$$

then $Z_\pm > 1$, and $W_\pm$ is given by

$$W_\pm=\frac{1}{2\eta_\pm}\ln\frac{16}{[1-\Phi+(t_{12}/\tau_c^{12})^2]}, \quad (6.35)$$

and decreases with increasing t_{12}. Consequently, $W_\pm$ reaches its maximum for

$$t_{12}^{\max}\approx\tau_c^{12}\left[\frac{n^2}{\eta_\pm^2}-(1-\Phi)\right]^{1/2}. \quad (6.36)$$

If the pulses have very different intensities ($\alpha_{\max}\gg\alpha_{\min}$ or $\beta\ll 1$), the asymmetrical part of the signal W_{AS} can be neglected, since $W_{AS}\ll\beta/\eta\ll\eta^{-1}$ (see Appendix D). Thus the signal is completely determined by its symmetrical part W_S. The condition $\beta\ll 1$ holds when $\eta_+\approx\eta_-\approx\eta$; in this limit $W_+\approx W_-$, and the signal, obtained from Eqs. (6.29)–(6.35), exhibit a peak centered at $t_{12}=0$. The peak has temporal width $|t_{12}|\approx\tau_c^{12}$ and, moreover, for fully correlated pulses ($\Phi=1$) there is an *additional* very narrow dip that appears in the middle of this central peak. This dip has width $|t_{12}|\approx(n/\eta)\tau_c^{12}$, depth $\sim 0.02\eta^{-1}$, and is very sensitive to the degree of mutual correlation of the pulses, since the dip vanishes as soon as $(1-\Phi)>n^2/\eta^2$, as shown in Fig. 4. For fully correlated pulses, the peak is approximately $2\pi^{-1}\ln(2\eta/n)$ times higher than the background signal [see Eq. (D17)]:

$$W_n^{(3)}(|t_{12}|\gg\tau_c^{12})=\frac{1}{3\eta\sqrt{2\pi}}\ , \quad (6.37)$$

which is reached for $|t_{12}|>\tau_c^{12}$ and which would be obtained for noncorrelated pulses [$\Phi=0$, see Eq. (6.21) for $n\ll\eta$].

In Fig. 6 the signal for order $n=1$ is shown as a function of intensity of the weaker pulse. The transition from a dip of width τ_c^{12} [$\alpha_{\min}t_p\ll 1$; Eq. (6.14)] to the peak ($1\ll\alpha_{\min}t_p\ll\alpha_{\max}t_p$) occurs for $\alpha_{\min}t_p\approx 1$. The absolute intensity of the background signal varies with $\alpha_{\min}t_p$ as

$$W_1^{(3)}=\tfrac{1}{3}\exp\left[-\frac{4\alpha_{\min}t_p}{3}\right]I_1\left[\frac{4\alpha_{\min}t_p}{3}\right], \quad (6.38)$$

where I_1 is a modified Bessel function, and reaches its maximum 0.07 for $\alpha_{\min}t_p=1.1$.

If the pulses have nearly equal intensities, such that

$$1-\beta=[(\alpha_1)^{1/2}-(\alpha_2)^{1/2}]^2/(\alpha_1+\alpha_2)\ll 1\ ,$$

one can see from Eq. (6.30) that $W_+\gg W_-$ and thus $W_S\approx W_+$. The asymmetrical part W_{AS} of the signal is still small. However, it cannot be neglected if the pulses are fully correlated [$(1-\Phi)<n^2/\eta^2\ll 1$] and the Doppler width of the atomic ensemble is large ($D\ll 1$).

In this case W_{AS} is given by

$$W_{AS}=\frac{2nG}{3\pi^2(4n^2-1)}\left[-D+\frac{8G^2\eta^2}{3}\right],\ \text{if } |G|\ll\eta^{-1}\ , \quad (6.39)$$

$$W_{AS}=\frac{G}{6\pi n\sqrt{\pi}},\ \text{if } \eta^{-1}\ll|G|\ll n\eta^{-1}\ , \quad (6.40)$$

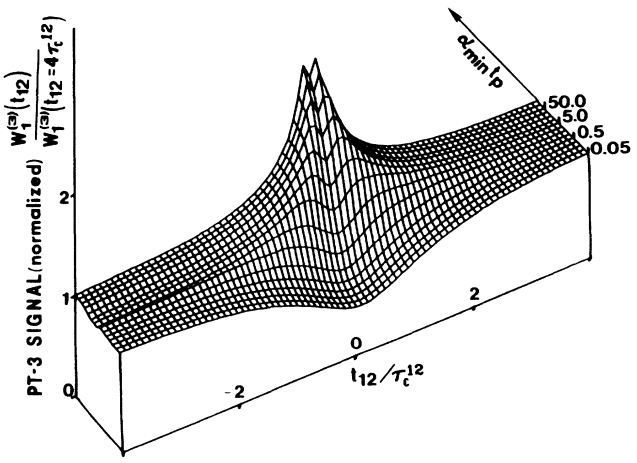

FIG. 6. Signal of order $n=1$ as a function of t_{12}/τ_c^{12} and $\alpha_{\min}t_p$ in a weak-relaxation limit in the case when one of the fully correlated ($\Phi=1$) pulses is strong $\alpha_{\max}t_p=500$, while the intensity of another varies, $0.05<\alpha_{\min}t_p<170$; $\Delta_D t_p=7$.

$$W_{\rm AS}=\frac{1}{3\pi\eta G\sqrt{\pi}}\left[y_0+\frac{2n}{\eta\sqrt{\pi}}\ln\frac{2|G|}{y_0+(y_0^2+2G^2D)^{1/2}}\right],\quad \text{if } n\eta^{-1}\ll|G|\ , \tag{6.41}$$

where

$$y_0=\frac{n}{\eta}\exp\left[-\frac{DG^2\eta^2}{n^2}\right].$$

One can see from Eqs. (6.39)–(6.41) that $W_{\rm AS}$ is much smaller than $W_{\rm S}$. However, when $|t_{12}|\le(n/\eta)\tau_c^{12}$, $W_{\rm AS}$ is comparable with the part of $W_{\rm S}$ which depends on delay time [see Eq. (6.33)]. As a result, the narrow dip in the middle of the peak practically vanishes (see Fig. 7) and the maximum of the signal shifts to

$$t_{12}^{\max}\approx\frac{n}{\eta}\tau_c^{12}\ .$$

For $|t_{12}|>\tau_c^{12}$ the signal reaches its background value given by

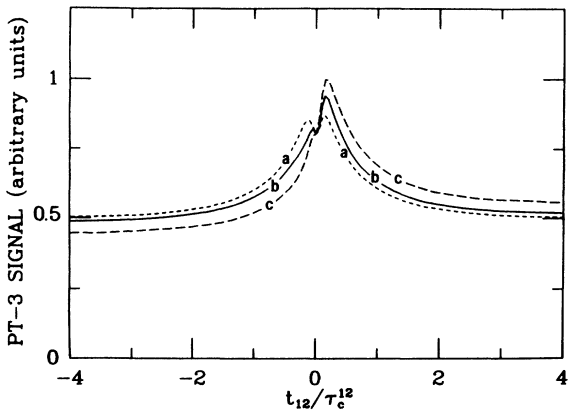

FIG. 7. Signals corresponding to order $n=1$ vs t_{12}/τ_c^{12} in a weak-relaxation limit in the case of fully correlated ($\Phi=1$) strong pulses with almost equal intensities ($\alpha_1 t_p=120$, $\alpha_2 t_p=100$) for different Doppler widths of the atomic ensemble: curve a, $-\Delta_D t_p=1.4$ ($D=118$); curve b, $-\Delta_D t_p=14$ ($D=1.2$); curve c, $-\Delta_D t_p=70$ ($D=0.05$).

$$W_n^{(3)}(|t_{12}|\gg\tau_c^{12})=\frac{1}{3\pi\eta\sqrt{2\pi}}\left[2\sqrt{2}+s\frac{n}{\eta\sqrt{2}}\ln\left\{\min\left[\left[\frac{\eta e}{n}\right]^2,\frac{2}{D}\right]\right\}\right], \tag{6.42}$$

where s is defined by Eq. (2.21). Comparing Eqs. (6.37) and (6.42), one can see that even in the case of equal intensities of the fully correlated pulses the background signal differs only slightly from that corresponding to noncorrelated pulses.

In Fig. 8 for $\alpha_1/\alpha_2=\text{const}\approx1$ the evolution of the signal with increasing intensity of both pulses is shown. The transition from the signal with no dependence on t_{12} [weak-field regime, $\alpha_{1,2}t_p\ll1$; Eq. (6.7)] to the signal with a well-defined peak (strong-field regime, $1\ll\alpha_{1,2}t_p$) occurs in the intermediate range of intensities; that is, when $\alpha_{1,2}t_p\approx1$. For these intensities the asymmetry of the signal and its absolute intensity reach their maximum values.

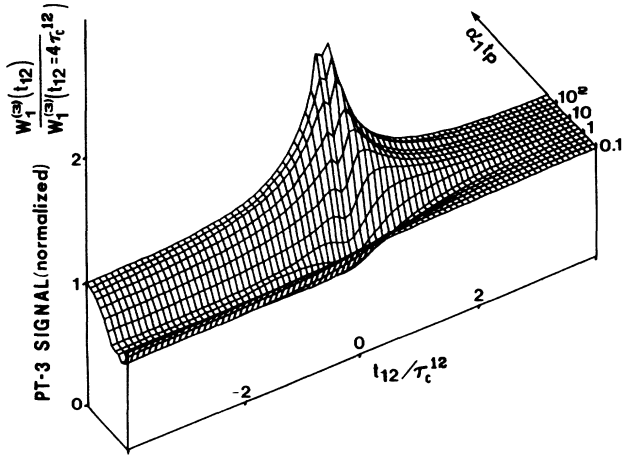

FIG. 8. Signal of order $n=1$ as a function of t_{12}/τ_c^{12} and $\alpha_1 t_p$ in a weak-relaxation limit; $\Delta_D t_p=7$. The fully correlated ($\Phi=1$) pulses have nearly equal intensities $\alpha_2/\alpha_1=1.2$ that vary from small to large values ($0.1<\alpha_1 t_p<500$).

The above discussion is valid for orders n satisfying $0<n\ll\eta$. The signal of order $n=0$ is difficult to detect, as it is emitted simultaneously with the third pulse in the same direction, but it is the strongest of the PT-3 signals. It is given completely by its symmetrical part, and at zero delay time can be expressed as

$$W_0^{(3)}(t_{12}=0)=W_1^{(3)}(t_{12}=0)+\frac{1}{3\eta\sqrt{2\pi}}\ . \tag{6.43}$$

For $t_{12}>\tau_c^{12}[n^2/2\eta_\pm^2-(1-\Phi)]^{1/2}$, the difference between PT-3 signals of zero and first order vanishes, and $W_0^{(3)}(t_{12})$ coincides with the symmetrical part of the signal $W_1^{(3)}(t_{12})$ given by Eq. (6.35). The zero-order signal always decreases with increasing $|t_{12}|$.

Let us now consider the PT-3 signals of higher order, that is, with $n\gg\eta$. These signals are relatively weak; nevertheless, they have some features that deserve discussion. For the sake of simplicity we consider fully correlated pulses ($\Phi=1$) in two limiting cases: (1) the pulses have very different intensities $\alpha_{\max}\gg\alpha_{\min}$, and (2) the pulses have equal intensities $\alpha_1=\alpha_2=\alpha$.

In the first case ($\alpha_{\max}\gg\alpha_{\min}$), if

$$\frac{n^4\alpha_{\min}}{\eta^4\alpha_{\max}} \ll 1 , \tag{6.44}$$

the signal is given by

$$W_n^{(3)}(t_{12}) = \frac{1}{3\eta\sqrt{2\pi}} \exp\left[-\frac{n^2(3-G^2)}{4\eta^2} \right] \times I_0\left[\frac{n^2(1-G^2)}{4\eta^2} \right] , \tag{6.45}$$

where I_0 is a modified Bessel function. As shown in Fig. 9, the signal (6.45) exhibits a profound dip of relative depth $|S| = (1-2\eta/\pi n) \approx 1$ centered at $t_{12}=0$; for $|t_{12}| > \tau_c^{12}$ the signal practically coincides with that for noncorrelated pulses.

When

$$\frac{n^4\alpha_{\min}}{\eta^4\alpha_{\max}} > 1 , \tag{6.46}$$

the background signal acquires a negative asymmetry if $D\eta^2/n^2 < 1$ [see Eq. (D36)].

In the second case (equal pulse intensities) the signal is given approximately by

$$W_n^{(3)} = \frac{\eta}{3\pi n^2\sqrt{\pi}} \left[|G| - G \operatorname{erf}\left[\frac{n}{\eta[2(DG^2+2)]^{1/2}} \right] \right] + \frac{\sqrt{2}\exp(-n^2/4\eta^2)}{3\pi n} \left[1 - \operatorname{erf}\left[\frac{n|G|}{4\eta} \right] \right] , \tag{6.47}$$

where erf is the error function.[43]

If the Doppler width of the atomic ensemble is sufficiently small, such that

$$\frac{n^2}{D\eta^2} = \left[\frac{n\Delta_D}{\alpha} \right]^2 \ll 1 , \tag{6.48}$$

then, as in the first limit ($\alpha_{\max} \gg \alpha_{\min}$), the PT-3 signal for equal intensities exhibits a dip whose minimum is shifted to positive t_{12}. The dip has relative depth close to unity, since the background signal

$$W_n^{(3)}(t_{12} > \tau_c^{12}) = \frac{\eta}{3n^2\pi\sqrt{\pi}} \tag{6.49}$$

is much larger than the value at zero delay time.

If the Doppler width is sufficiently large, such that condition (6.48) is violated, the signal (6.47) becomes strongly negatively asymmetric and the dip vanishes (see Fig. 10).

The remarkable feature of Eq. (6.49) is the power-law-type dependence of the signal on n for $t_{12} > \tau_c^{12}$, rather than the Gaussian-like dependence seen in Eq. (6.45) for pulses having different intensities. As a result, it may be easier to detect signals corresponding to large n if equal pulse intensities are used. By comparing Eqs. (6.49) and (6.21), one sees that the background signal for equal intensity, fully correlated pulses differs from that for noncorrelated pulses. This is the only limit where such a marked deviation occurs; the origin of this effect can be traced to the increasing importance of the α_{12} term in the denominator of Eq. (6.10), a term that was ignored in the qualitative discussion following that equation.

When both fields are strong, the PT-3 signal differs in almost every respect from the analogous signal in the weak-field regime. The strong-field PT-3 signals are emitted with comparable intensities in many directions (corresponding $n < n_0 \lesssim \eta$), while the weak-field signals only in the $\mathbf{k}_3 \pm \mathbf{k}_d$ directions. The signal for correlated pulses can be much stronger than that for noncorrelated in the strong-field regime but not in the weak-field regime. Only the strong-field result depends directly on the cross-correlation time τ_c^{12} exhibiting a well-defined narrow peak ($n \ll \eta$), dip ($n \gg \eta$), or combination of them ($n \sim \eta$) at $t_{12}=0$. A negative asymmetry of the signal also occurs only in a strong-field regime.

Finally, it is possible to show that, in sharp contrast to the weak-field regime, for strong fields the signal induced

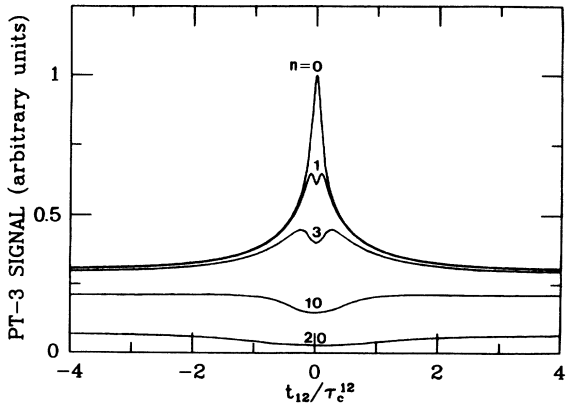

FIG. 9. Signals corresponding to different orders n vs t_{12}/τ_c^{12} in a weak-relaxation limit. Both pulses are strong and have very different intensities $\alpha_{\max}t_p = 10^4$, $\alpha_{\min}t_p = 100$ ($\beta = 0.2$); $\Delta_D t_p = 14$, $\Phi = 1$.

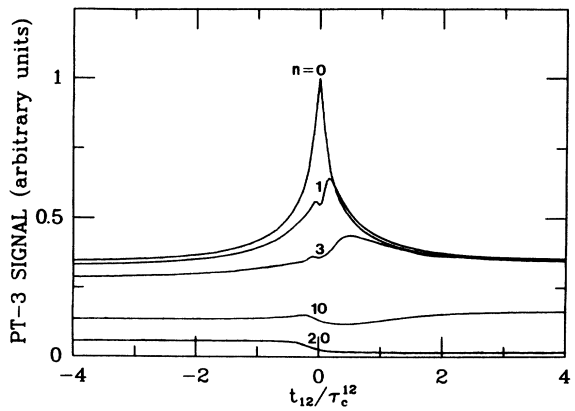

FIG. 10. Signals corresponding to different orders n vs t_{12}/τ_c^{12} in a weak-relaxation limit. Both pulses are strong and have nearly equal intensities $\alpha_{\max}t_p = 120$, $\alpha_{\min}t_p = 100$ ($\beta = 0.996$). All other parameters and notations are the same as in Fig. 9.

by the correlated pulses originates from the stochastic part of the population grating $[\rho_3^{(n)}(t_p)-\langle\rho_3^{(n)}(t_p)\rangle]$, while the contribution from the constant part of the grating, $\langle\rho^{(n)}(t_p)\rangle$, is negligible. In the weak-field regime, the constant and stochastic parts of the population grating induced by the fully correlated pulses provide signals of the same intensity [see Eqs. (6.6) and (6.7)]. To understand the strong-field results one can consider the mean amplitude $\rho^{(n)}=\langle\rho_3^{(n)}(t_p)\rangle$ for the grating of the order n.

Since the spontaneous relaxation is assumed to be negligible ($\gamma_l \ll t_p^{-1}$) we obtain from Eq. (5.3)

$$\rho^{(n)}=(-1)^n e^{-(\alpha_1+\alpha_2)t_p} I_n(2\alpha_{12}t_p) , \tag{6.50}$$

where I_n is a modified Bessel function. In contrast to the two-atom correlation function $T^{(n,-n)}=\langle\rho_3^{(n)}(t_p)\bar{\rho}_3^{(n)}(t_p)\rangle$, the single-atom amplitude (6.50) does not depend on either delay time t_{12} or the detuning δ.

As long as condition

$$(\alpha_1+\alpha_2-2\alpha_{12})t_p=\alpha(\pi)t_p \gg 1 \tag{6.51}$$

is satisfied [$\alpha(\phi)$ is defined in Eq. (4.5)], the mean grating amplitude $\rho^{(n)}(t_p)$ given by (6.50) is exponentially small for any n, namely

$$\rho^{(n)}(t_p) \ll e^{-(\alpha_1+\alpha_2-2\alpha_{12})t_p} \ll 1 .$$

However, if the pulses are almost fully correlated ($\Phi\approx 1$) with nearly equal intensities ($\alpha_1\approx\alpha_2\approx\alpha_{12}$), inequality (6.51) can be violated to the point that

$$(\alpha_1+\alpha_2-2\alpha_{12})t_p \lesssim 1 . \tag{6.52}$$

For $\max\{n,1\} \ll \alpha_{12}t_p$ it follows from Eq. (6.50) that

$$\rho^{(n)}(t_p)=\frac{(-1)^n \exp(-n^2/4\alpha_{12}t_p)}{(4\pi\alpha_{12}t_p)^{1/2}} \times e^{-(\alpha_1+\alpha_2-2\alpha_{12})t_p} , \tag{6.53}$$

and, owing to condition (6.52), the gratings characterized by $n<(2\alpha t_p)^{1/2}$ have nonexponentially small mean amplitudes $\sim(\alpha t_p)^{-1/2}$.

It is not too difficult to understand the physical origin of Eq. (6.51). The atoms in the sample see interference fringes produced by the excitation pulses. Atoms at points other than interference minima are saturated by the fields. If the pulse amplitudes are unequal, the intensity at the minima of the interference fringes is still sufficiently high (in the strong-field regime) to saturate even these atoms. These saturated atoms produce exponentially small contributions to the mean grating amplitude. On the other hand, for equal pulse amplitudes, atoms near the interference minima see an arbitrarily small effective total field; these atoms are not saturated. As a result, the mean amplitude $\rho(t_p;\phi)$ of the spatial population grating has narrow groves in the vicinity of the minima $\phi\approx(2m+1)\pi$ ($m=0,\pm1\ldots$) of the interference fringes.

If the nth-order population grating $\rho_3^{(n)}(t_p;\delta)$ is written as the sum of the constant and stochastic contributions,

$$\rho_3^{(n)}(t_p;\delta)=\rho^{(n)}(t_p)+[\rho_3^{(n)}(t_p)-\rho^{(n)}(t_p)] , \tag{6.54}$$

the correlation function $T^{(n,-n)}=\langle\rho_3^{(n)}(t_p;\delta)\rho_3^{(-n)}(t_p;\tilde{\delta})\rangle$ is given by

$$T^{(n,-n)}(t_p)=[\rho^{(n)}(t_p)]^2 + \langle[\rho_3^{(n)}(t_p;\delta)-\rho^{(n)}(t_p)] \times[\rho_3^{(-n)}(t_p;\tilde{\delta})-\rho^{(n)}(t_p)]\rangle . \tag{6.55}$$

We did not take into account the first term in Eq. (6.55) when deriving the results in the strong-field regime, owing to the fact that this contribution is (a) exponentially small if condition (6.52) is violated and (b) still small relative to the second term of Eq. (6.55) [compare Eqs. (6.53) and (6.49)] even if condition (6.52) is satisfied. In other words, for all $\alpha_1,\alpha_2,\alpha_{12}$, the signal in the strong-field regime is produced by the stochastic part of the populating grating, i.e.,

$$W_n^{(3)} \approx T^{(n,-n)}(t_p,\delta,\delta) \approx\langle|\rho_3^{(n)}(t_p;\delta)-\rho^{(n)}(t_p)|^2\rangle \gg [\rho^{(n)}(t_p)]^2 . \tag{6.56}$$

VII. QUALITATIVE EXPLANATION OF THE STRONG-FIELD RESULTS

To give a qualitative explanation of the strong-field results obtained in Sec. VI, we recall that the PT-3 signal depends directly on the correlation function $T(t_p)=\langle\rho_3(t_p;\phi,\delta)\rho_3(t_p;\tilde{\phi},\tilde{\delta})\rangle$ of population differences of two atoms. In general, these atoms are characterized by different positions ($\phi\neq\tilde{\phi}$) and velocities ($\delta\neq\tilde{\delta}$). More precisely, according to Eqs. (2.19), (2.20), and (2.23), the part of the signal symmetrical relative to t_{12} and n depends only on the correlation $\langle\rho_3(t_p;\phi,\delta)\rho_3(t_p;\tilde{\phi},\delta)\rangle$ of atoms having the same velocity. The asymmetrical part of the signal can arise when

$$\langle\rho_3(t_p;\phi,\delta)\rho_3(t_p;\tilde{\phi},\tilde{\delta})\rangle \neq \langle\rho_3(t_p;\tilde{\phi},\delta)\rho_3(t_p;\phi,\tilde{\delta})\rangle . \tag{7.1}$$

To explain the obtained results, we first consider the behavior of the correlation function $T(t_p)$ as a function of $\phi,\tilde{\phi},\delta,\tilde{\delta}$ and t_{12}. Since in a strong-field regime the population difference $\rho_3(t_p;\phi,\delta)$ is a stochastic quantity with $\langle\rho_3(t_p;\phi,\delta)\rangle\approx 0$, only those atoms that satisfy the condition $\rho_3(t_p;\phi,\delta)\approx\rho_3(t_p;\tilde{\phi},\tilde{\delta})$ contribute to the signal. To determine the range of ϕ and $\tilde{\phi}$ and δ and $\tilde{\delta}$ that contribute to $W_n^{(3)}(t_{12})$ for a given t_{12}, let us consider fully correlated excitation pulses ($\alpha_{12}=\sqrt{\alpha_1\alpha_2}$), when the PT-3 signal reveals the most profound dependence on t_{12}.

First we analyze the case of zero delay time, $t_{12}=0$. The behavior of the correlation function $T(t_p)$ depends implicitly on the spatial dependence of the incident fields, which in turn is represented by the total Rabi frequency $f(t,\phi)$. As the pulses are assumed to be fully correlated, $f(t,\phi)$ can be represented in the form

$$f(t,\phi)=f_1 e^{-i\phi}+f_2 = |f_1(t)|\left[\frac{\alpha(\phi)}{\alpha_1}\right]^{1/2}\exp\{i[\theta+\arg f_1(t)]\} , \tag{7.2}$$

where

$$\alpha(\phi)=\alpha_1+\alpha_2+2(\alpha_1\alpha_2)^{1/2}\cos(\phi)\ , \tag{7.3}$$

and

$$\tan\theta=-\frac{\alpha_1\sin\phi}{\alpha_1\cos\phi+(\alpha_1\alpha_2)^{1/2}}\ .$$

The phase θ does not depend on time and thus cannot affect the evolution of atomic population, while $\arg f_1(t)$ is the same for all atoms. Thus, all the essential dependence on ϕ is contained only in the absolute value of the Rabi frequency $|f(t,\phi)|$, which in turn represents a fixed spatial grating (or interference fringes) proportional to $\alpha(\phi)$, whose amplitude fluctuates in time according to $|f_1(t)|$.

The larger the difference in $|f(t,\phi)|$ and $|f(t,\tilde{\phi})|$ for atoms characterized by ϕ and $\tilde{\phi}$, the faster is the decorrelation of their populations. A difference in detunings (velocities) leads to the same decorrelation. Namely, for $\alpha(\phi)\approx\alpha(\tilde{\phi})$, only those atoms which satisfy the condition [see Eq. (C8)]

$$\tfrac{1}{3}(\sqrt{\alpha(\phi)}-\sqrt{\alpha(\tilde{\phi})})^2t_p+\frac{(\delta-\tilde{\delta})^2t_p}{3\alpha(\phi)}<1 \tag{7.4}$$

contribute to the signal. At $t_{12}=0$, however, the asymmetrical part of the signal vanishes, and only correlations between atoms with equal velocities are important. Thus, one need consider only the first term in Eq. (7.4) when $t_{12}=0$.

For $\alpha(\phi)\approx\alpha(\tilde{\phi})$, it follows from Eq. (7.3) one needs to have $\cos\phi\approx\cos\tilde{\phi}$. Consequently, the population correlations can be of two types. For a given atom, characterized by "location" $\phi=\mathbf{k}_d\cdot\mathbf{r}(-\pi/2\le\phi\le3\pi/2)$, the first type of correlation occurs with a neighboring atom having

$$\tilde{\phi}\approx\phi\ . \tag{7.5}$$

The second type of correlation arises for an atom located at ϕ and another one at

$$\begin{aligned}&\tilde{\phi}\approx-\phi,\quad \text{if } -\frac{\pi}{2}\le\phi\le\frac{\pi}{2}\ ,\\ &\tilde{\phi}\approx2\pi-\phi,\quad \text{if } \frac{\pi}{2}\le\phi\le\frac{3\pi}{2}\ .\end{aligned} \tag{7.6}$$

These correlations are illustrated qualitatively in Fig. 11. According to Eqs. (7.5) and (7.6), all atoms are naturally separated into two subensembles: those which are closer to maxima $-\pi/2\le\phi<\pi/2$ or minima $\pi/2\le\phi<3\pi/2$ of the interference fringes, respectively. The atomic populations are correlated only within these subensembles, which therefore contribute to the PT-3 signal independently:

$$W_n^{(3)}=W_{n,\max}^{(3)}+W_{n,\min}^{(3)}\ , \tag{7.7}$$

where max and min designate "maxima" and "minima" subensembles, respectively.

To continue the analysis, one must distinguish between two limiting cases, that of (1) pulses with very different intensities ($\alpha_{\max}\gg\alpha_{\min}$), and (2) pulses with nearly equal intensities ($\alpha_1\approx\alpha_2$). In the first case one can see from Fig. 11(a) that the spatial modulation of the interference fringes is small compared with its average amplitude. Hence, one can expect the behavior of the correlation function $T(t_p)$ to be almost identical for the "maxima" and "minima" subensembles. In the second case the "minima" subensemble is driven by a considerably weaker field than the "maxima" one [see Fig. 11(b)]; this can result in different contributions to $T(t_p)$ from the two subensembles.

If the pulses have very different intensities, condition (7.4) takes the form ($\delta=\tilde{\delta}$)

$$\frac{\alpha_{\min}t_p}{3}(\cos\phi-\cos\tilde{\phi})^2<1\ . \tag{7.8}$$

The fact that expression (7.8) is not changed under the substitution $\phi\to\phi+\pi$; $\tilde{\phi}\to\tilde{\phi}+\pi$ proves the behavior of $T(t_p)$ to be identical for the two subensembles. Suppose

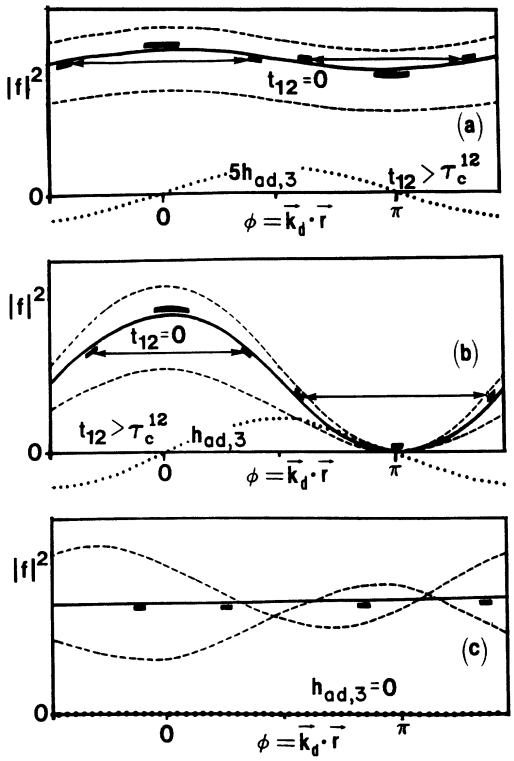

FIG. 11. Schematic representation of the two types of population correlations for $t_{12}=0$ for different excitation pulses. (a) The pulses are strong, fully correlated, and have very different intensities. Rectangles depict the range of correlations of the first type, while arrows depict the correlations of the second type. The solid curve represents the averaged interference fringes $\langle|f(t)|^2\rangle$, while the dashed curves depict nonaveraged interference fringes $|f(t)|^2$ for two different times. The effective detuning, which arises at $t_{12}\neq0$, is shown by the dotted curve. (b) The pulses have equal intensities. All other conditions and notations are the same as in (a). (c) The pulses are noncorrelated; only the correlations of the first type exist, and the effective detuning vanishes.

an atom is located near an extremum of the interference fringes ($\phi \approx 0$ or $\phi \approx \pi$). Then, $\tilde{\phi} \approx \phi$ holds for the both types of population correlations. Since $\sqrt{\alpha(\phi)}$ varies slowly near extrema, the amount of $(\phi - \tilde{\phi})$ that can still contribute to $T(t_p)$ is relatively large. According to Eq. (7.8) this range is given by

$$|\phi - \tilde{\phi}| < (\alpha_{\min} t_p)^{-0.25} \ll 1 . \tag{7.9}$$

On the other hand, if an atom characterized by ϕ is located at a slope of the interference fringes, then the correlations of the different types are well separated in space, and only the atoms satisfying

$$|\phi - \tilde{\phi}| < (\alpha_{\min} t_p)^{-0.5} \ll 1$$

(first type of correlations) (7.10)

and

$$|\phi + \tilde{\phi}| < (\alpha_{\min} t_p)^{-0.5} \ll 1 ,$$
$$|\phi + \tilde{\phi} - 2\pi| < (\alpha_{\min} t_p)^{-0.5} \ll 1 , \tag{7.11}$$

(second type of correlations)

can contribute to the signal. The ranges (7.10) and (7.11) are much smaller than (7.9).

For pulses with equal intensities ($\alpha_1 = \alpha_2 = \alpha$), condition (7.4) for atoms to contribute is

$$\frac{4\alpha t_p}{3} \left[\cos\frac{\phi}{2} - \cos\frac{\tilde{\phi}}{2} \right]^2 < 1 . \tag{7.12}$$

Comparing Eqs. (7.8) and (7.12), one finds that for the "maxima" subensemble, the behavior of correlations is not changed significantly compared to the case $\alpha_{\max} \gg \alpha_{\min}$. However, for the "minima" subensemble, that is, for an atom located close to a minimum of the interference fringes ($\phi \approx \pi$), the amount of $(\phi - \tilde{\phi})$ that can still lead to a contribution to $T(t_p)$ decreases drastically. According to Eq. (7.12), this range is given by

$$|\phi - \tilde{\phi}| < (\alpha t_p)^{-0.5} \ll 1 , \tag{7.13}$$

and does not differ from that of an atom located at a slope of the interference fringes.

To consider what happens to the population correlations when the pulses become time delayed ($t_{12} \neq 0$), we use the model developed in Sec. III, in which, for $0 < t_{12} \ll \alpha_{1,2}^{-1}$, the pulses can be still regarded as fully overlapping and the Rabi frequency, $f(t,\phi)$, is still given by Eq. (7.2). In this model, every two-level atom acquires an additional detuning $h_{\text{ad},3}(\phi) = G(t_{12})(\alpha_1 \alpha_2)^{1/2} \sin\phi$; consequently, the second term in Eq. (7.4) is modified, and the condition for atoms to contribute to $T(t_p)$ becomes

$$\tfrac{1}{3}[\sqrt{\alpha(\phi)} - \sqrt{\alpha(\tilde{\phi})}]^2 t_p + \frac{[\delta - \tilde{\delta} + h_{\text{ad},3}(\phi) - h_{\text{ad},3}(\tilde{\phi})]^2 t_p}{3\alpha(\phi)} < 1 . \tag{7.14}$$

The additional ϕ-dependent detuning alters the symmetrical part of the signal since it results in an additional dephasing for atoms having equal detunings $\delta = \tilde{\delta}$. First one notes that the additional detuning varies as $\sin\phi$ (see Fig. 11). This implies that correlations of the type 2 for atoms located at the slopes of the interference fringes are destroyed for relatively small values of t_{12}. For example, for the atoms characterized by $\phi \approx -\tilde{\phi} \approx \pi/2$ and $\phi \approx 2\pi - \tilde{\phi} \approx \pi/2$ the difference in additional detunings [see Eq. (7.14)] is maximal, and the correlation of their populations is already destroyed at $t_{12} \approx \tau_c^{12}/(\alpha_{\min} t_p)^{1/2} \ll \tau_c^{12}$. For larger delay time and pulses having very different intensities, the range $(\phi - \tilde{\phi})$ that contributes to the signal for the atoms located in the vicinity of the extrema of the interference fringes decreases from $(\alpha_{\min} t_p)^{-0.25}$ to $(\alpha_{\min} t_p)^{-0.5}$ as t_{12} varies from 0 to $t_{12} \gg \tau_c^{12}$. For $t_{12} > \tau_c^{12}$ the range $(\phi - \tilde{\phi})$ which contributes to the signal is the same for atoms at the extrema and the slopes of the interference fringes (in contrast to the situation at $t_{12} = 0$). This result also holds for atoms near the maxima in the case of equal pulse intensities. However, the range $(\phi - \tilde{\phi})$ of the correlations for the atoms near the minima ($\phi \approx \pi$) shrinks from the value (7.13) to an even smaller value $\cos(\phi/2)(\alpha t_p)^{-0.5}$.

In general, when $\alpha(\phi) \approx \alpha(\tilde{\phi})$, the detuning term [second term of Eq. (7.14)] leads to eventual decorrelation for $t_{12} \neq 0$. However, for certain unequal detunings $\delta \neq \tilde{\delta}$, this decorrelation can be significantly reduced. If

$$\delta - \tilde{\delta} \approx h_{\text{ad},3}(\tilde{\phi}) - h_{\text{ad},3}(\phi) \tag{7.15}$$

the second term of Eq. (7.14) vanishes and the correlation of the populations coincides with that for the atoms with equal detunings at $t_{12} = 0$. For detunings $\delta \neq \tilde{\delta}$ which satisfy (7.15), there is always a contribution to the asymmetrical part of the signal.

The analysis of the population correlations presented above and the representation of the atomic ensemble as a sum of "maxima" and "minima" subensembles helps to explain the dependence of the signal on time delay t_{12} and grating order N. First, using Eq. (7.7), one can show that, owing to Eqs. (2.19), (2.23), and (6.9), the total PT-3 signals emitted in all directions by these subensembles are given by

$$\sum_{n=-\infty}^{\infty} W_{n,\max}^{(3)} = \sum_{n=-\infty}^{\infty} W_{n,\min}^{(3)} = \tfrac{1}{6} , \tag{7.16}$$

such that the total signal satisfies

$$\sum_{n=-\infty}^{\infty} W_n^{(3)} = \tfrac{1}{3} . \tag{7.17}$$

The sum rules (7.16) and (7.17) are valid independent of the delay time or correlation properties of the pulses. For any given delay time t_{12} and correlation parameter Φ, one can regard $W_{n,\max}^{(3)}$, $W_{n,\min}^{(3)}$, and $W_n^{(3)}$ as some "distribution" functions of the signal intensity relative to N. Consequently, knowledge of $W_n^{(3)}(t_{12})$ for a given n allows one to draw conclusions about $W_n^{(3)}(t_{12})$ for other values of n.

A. Pulses with very different intensities

In this case it has been shown that at $t_{12}=0$ the behavior of $T(t_p)$ in both ("maxima" and "minima") subensembles is identical [see Fig. 12(a)], and thus

$$W^{(3)}_{n,\max}(t_{12}=0)=W^{(3)}_{n,\min}(t_{12}=0)=0.5W^{(3)}_{n}(t_{12}=0)\ ,$$

where, according to Eqs. (2.23) and (2.19), $W^{(3)}_n$ is given by

$$W^{(3)}_n(0)=T^{(n,-n)}(t_p,\delta,\delta)=\frac{1}{4\pi^2}\int_{-\pi/2}^{3\pi/2}d\phi\int_{-\pi/2}^{3\pi/2}d\tilde{\phi}\langle\rho_3(t_p,\phi,\delta)\rho_3(t_p,\tilde{\phi},\delta)\rangle\cos n(\phi-\tilde{\phi})\ . \tag{7.18}$$

The correlation function appearing in Eq. (7.18) is always positive, as is $W^{(3)}_0$. Owing to the oscillatory behavior of $\cos n(\phi-\tilde{\phi})$ for $n\neq 0$ the distribution $W^{(3)}_n(t_{12}=0)$ is a smoothly decreasing symmetrical function of n, characterized by width n_0 with $n_0\gg 1$.

For $t_{12}>0$ the two subensembles lead to the distributions $W^{(3)}_{n,\max}(t_{12})$ and $W^{(3)}_{n,\min}(t_{12})$ which acquire some asymmetry [see Fig. 12(b) and Eq. (7.15)]. However, the asymmetry of the "maxima" distribution is positive [$W^{(3)}_{n,\max}(t_{12})>W^{(3)}_{-n,\max}(t_{12})$], while that of the "minima" is negative, such that they are exactly compensated in the joint "distribution" $W^{(3)}_n(t_{12})$, which is symmetrical relative to n (and t_{12}).

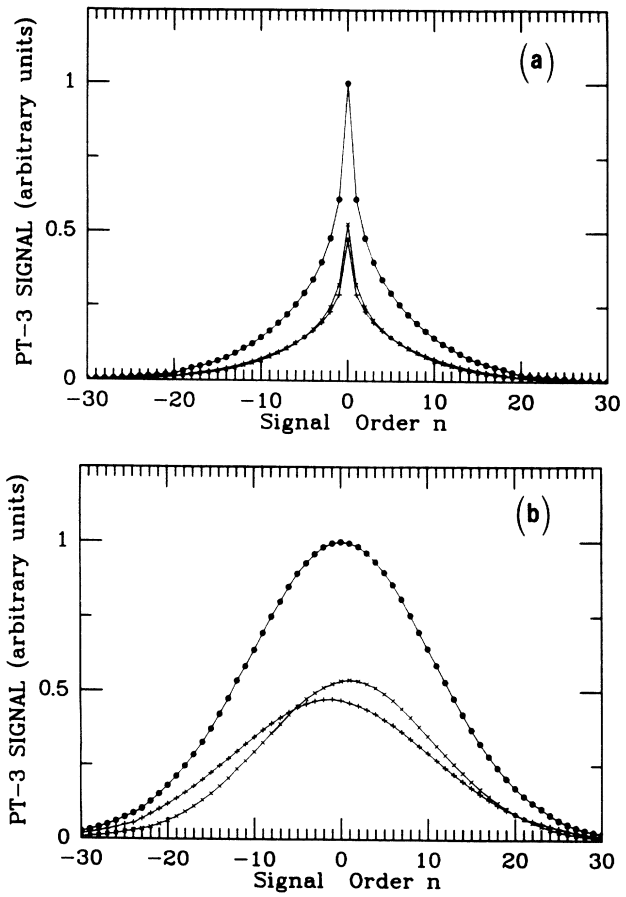

FIG. 12. Distribution of the signal intensity as a function of order N for delay time (a) $t_{12}=0$ and (b) $t_{12}=2\tau_c^{12}$ ●, the total signal intensity $W^{(3)}_n$; +, the signal intensity $W_{n,\min}$ corresponding to the "minima" ensemble; ×, the signal intensity $W_{n,\max}$ corresponding to the "maxima" ensemble ($W^{(3)}_n=W_{n,\min}+W_{n,\max}$). The pulses are fully correlated and have very different intensities: $\Phi=1$, $\alpha_1 t_p=10^4$, $\alpha_2 t_p=10^2$, $\Delta_D t_p=14$.

Some insight into $W^{(3)}_n(t_{12})$ can be obtained by first considering $W^{(3)}_0(t_{12})$. In light of the discussion above about the destruction of correlations with increasing t_{12}, one finds that the signal $W^{(3)}_0(t_{12}\neq 0)<W^{(3)}_0(0)$. When t_{12} becomes larger than τ_c^{12}, only the correlations of the first type survive, and the signal $W^{(3)}_0(t_{12})$ tends to its minimum, $W^{(3)}_0(\infty)$. Thus, the signal $W^{(3)}_0(t_{12})$ exhibits a peak of width τ_c^{12} [see Figs. 8–10 and the discussion that follows Eq. (6.43)].

To see the connection between $W^{(3)}_n(T_{12})$ ($n\neq 0$) and $W^{(3)}_0(t_{12})$, one can use the fact that in the strong-field regime the number n_0 of the PT-3 signals of comparable intensity is large, and owing to relation (7.17) can be expressed as

$$n_0(t_{12})\sim[W^{(3)}_0(t_{12})]^{-1}\ . \tag{7.19}$$

Since the signal $W^{(3)}_0$ decreases with increasing t_{12}, it follows that n_0 increases with increasing t_{12} (in the limit $\alpha_{1,2}t_{12}\ll 1$ considered in this paper), i.e., $n_0(0)=n_0(t_{12}=0)<n_0(\infty)=n(t_{12}\gg\tau_c^{12})$. Now it is possible to get a qualitative understanding of the dependence of the signal $W^{(3)}_n$ with a given n on t_{12}. As t_{12} varies from 0 to $t_{12}>\tau_c^{12}$, n_0 rises from $n_0(0)$ to $n_0(\infty)$ and the "distribution" function $W^{(3)}_n$ becomes wider and, consequently, lower in the center (small n) and higher at the wings (large n) (see Fig. 12). For fixed $n\lesssim n_0(0)$, $W^{(3)}_n$ decreases with increasing t_{12}, while for $n\gtrsim n_0(\infty)$, the signal $W^{(3)}_n$ increases with increasing t_{12}. Thus in the former case there is a peak centered at t_{12} and in the latter case a dip. In the intermediate range of n, $n_0(0)<n<n_0(\infty)$, the signal first increases and then decreases with increasing t_{12}. For $t_{12}>\tau_c^{12}$ the signal $W^{(3)}_n$ reaches the background value shown in Fig. 12(b). The narrow dip in the central peak that can occur for fully correlated pulses and small n can be traced to the fact that at $t_{12}=0$ the contribution of the correlations of the second type to the signal is negative, and they are destroyed on a time scale $t_{12}\ll\tau_c^{12}$. For example, at $t_{12}=0$ this contribution to the first-order signal $W^{(3)}_1$ is characterized by $(\phi-\tilde{\phi})\approx\pi$ and is negative as $\cos(\phi-\tilde{\phi})\approx-1$ in Eq. (7.18). Since these correlations are destroyed as t_{12}

varies from 0 to $t_{12}\approx\tau_c^{12}/(\alpha_{\min}t_p)^{1/2}$, this leads to the dip in the central peak having this width.

B. Pulses with equal intensities

In this case the behavior of $T(t_p)$ is different for the two subensembles even at $t_{12}=0$ [see Fig. 11(b)], and consequently $W^{(3)}_{n,\max}(t_{12}=0)\neq W^{(3)}_{n,\min}(t_{12}=0)$. As these signals represent Fourier transforms (phase factor $\exp[in(\phi-\tilde{\phi})]$) of $T(t_p)$, and, as discussed previously, the range of $(\phi-\tilde{\phi})$ that contributes to the signal is much narrower for the "minima" subensemble, it follows that the distribution $W^{(3)}_{n,\min}(t_{12}=0)$ over n is much wider and lower than $W^{(3)}_{n,\max}(t_{12}=0)$; that is, $n_{0,\min}(t_{12}=0)\gg n_{0,\max}(t_{12}=0)$ [see Fig. 13(a)]. Hence, $W^{(3)}_{n,\max}(t_{12}=0)$ and $W^{(3)}_{n,\min}(t_{12}=0)$ determines the signals of small and high orders, respectively. As in the case of pulses with very different intensities, the distributions $W^{(3)}_{n,\max}(t_{12})$ and $W^{(3)}_{n,\min}(t_{12})$ acquire some positive and negative asymmetry, respectively, as t_{12} increases. However, the asymmetrical parts of these signals are not canceled in $W^{(3)}_n(t_{12})$. As t_{12} tends from 0 to $t_{12}\gg\tau_c^{12}$, both "distributions" become wider and lower, and the relation $n_{0,\min}(t_{12})>n_{0,\max}(t_{12})$ is satisfied for any t_{12} [see Fig. 13(b)]. As a result, the signal of small order n is still determined by the "maxima" distribution $[W^{(3)}_n(t_{12})\approx W^{(3)}_{n,\max}(t_{12})]$ and has positive asymmetry, while that of high order is determined by the "minima" distribution and has negative asymmetry. When the Doppler width is sufficiently large such that

$$\Delta_D\gg\left[\frac{\alpha}{t_p}\right]^{1/2},$$

condition (7.15) can be satisfied in the whole range of $\phi-\tilde{\phi}$ contributing to the signal, and the asymmetry becomes most visible.

In the opposite limiting case of noncorrelated pulses, the position as well as the amplitude of interference fringes varies in time [see Fig. 11(c)]. Therefore only the first type of the population correlations exists at $t_{12}=0$. Moreover, the additional detuning vanishs, and nothing changes for $t_{12}\neq0$ as compared with the case of zero delay time. As a result, $W^{(3)}_0(t_{12})\equiv W^{(3)}_0(0)$ and does not vary with t_{12}.

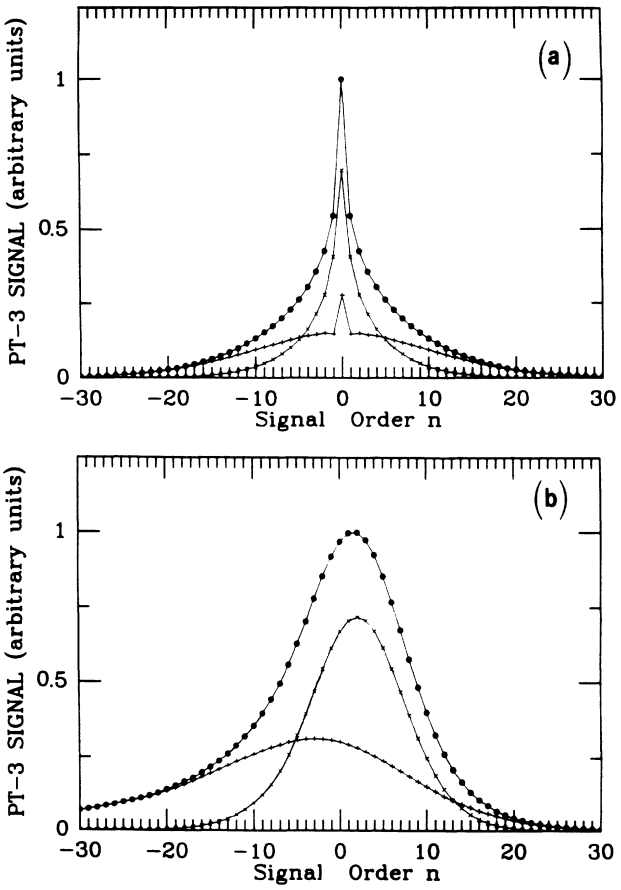

FIG. 13. Distribution of the signal intensity as a function of order n for different delay times: (a) $-t_{12}=0$; (b) $-t_{12}=2\tau_c^{12}$. The fully correlated pulses ($\Phi=1$) have nearly equal intensities ($\alpha_1t_p=105$, $\alpha_2t_p=100$), and $\Delta_Dt_p=14$. All the notations are the same as in Fig. 12.

C. Dephasing of two Bloch vectors

Up to now, we have been concerned with the signal as a function of t_{12} for fixed t_p. One can also try to understand the qualitative behavior of the correlation function $T(t_p)=\langle\rho_3\tilde{\rho}_3\rangle$ as a function of t_p for fixed t_{12}. Explicitly, $T(t_p)=\exp\{\lambda_1t_p\}/3$ [see Eqs. (6.9) and (6.10)] and leads to all the results for the PT-3 signal discussed in Sec. VI. This correlation function describes the relative dephasing of the components ρ_3 and $\tilde{\rho}_3$ of two Bloch vectors, $\mathbf{R}$ and $\tilde{\mathbf{R}}$, associated with two-level atoms having different velocities and spatial positions, $\mathbf{r}$ and $\tilde{\mathbf{r}}$, such that

$$\delta\neq\tilde{\delta}\quad\text{and}\quad\phi=\phi(\mathbf{r})\neq\phi(\tilde{\mathbf{r}})=\tilde{\phi}\ . \tag{7.20}$$

To understand the origin of Eq. (6.9), we examine the rotation of $\mathbf{R}$ and $\tilde{\mathbf{R}}$ using the model discussed in Sec. III. We consider the excitation pulses to be fully overlapping and take into account a nonzero delay time by introducing an additional detuning $h_{\mathrm{ad},3}(t_{12},\phi)$ given by Eq. (3.10). It follows from condition (7.20) that, generally speaking, $h_{\mathrm{ad},3}\neq\tilde{h}_{\mathrm{ad},3}$. Hence, even if two atoms have equal velocities, their effective detunings differ if they are located at different spatial points. Moreover, these atoms see different field amplitudes at different spatial locations.

First we consider the Bloch vector $\mathbf{R}$. It rotates with the angular velocity $\mathbf{H}$ given by

$$\mathbf{H}=\begin{bmatrix}X\\Y\\-(\delta+h_{\mathrm{ad},3})\end{bmatrix}, \tag{7.21}$$

[see Eq. (3.6)], where X and Y are the real and imaginary parts of the Rabi frequency $f(t)$ associated with a total electric field, $X+iY=-f(t)$, and the atom-field detuning δ is modified by the addition of $h_{\mathrm{ad},3}$. For the remainder of this section we assume that $\tau_c^{ij}=\tau_c;i,j=1,2$.

Owing to the fluctuating character of the angular ve-

locity components X and Y, the Bloch vector $\mathbf{R}$ rotates randomly and its tip undergoes a fast, random walk movement over the sphere having unit radius. This stochastic movement is superimposed on the free precession of the Bloch vector about the 3 axis with the constant angular velocity $-(\delta+h_{\mathrm{ad},3})$. By moving from the "absolute" reference frame, where the angular velocity is given by $\mathbf{H}$, into the reference frame that rotates about the 3 axis with angular velocity $-(\delta+h_{\mathrm{ad},3})$, one transforms away this regular rotation. In the new reference frame the component of the vector $\mathbf{H}$ along the 3 axis is zero and the X and Y components are modified. However, if

$$(\delta+h_{\mathrm{ad},3})\tau_c \ll 1 , \tag{7.22}$$

the modification of X and Y can be neglected. In the following discussion the analysis of the rotation of the vector $\mathbf{R}$ is carried out with respect to the rotating reference frame.

During time interval τ_c, X, and Y can be considered as constant, and the Bloch vector $\mathbf{R}$ deviates from its initial position $\mathbf{R}(t)$ by a small angle

$$\chi(\tau_c)\sim(X^2+Y^2)^{1/2}\tau_c \ll 1 . \tag{7.23}$$

The rotation occurring within the next interval of duration τ_c is independent of any previous one. According to the random walk model, after m such rotations, at time $t_1=m\tau_c$ the Bloch vector $\mathbf{R}(t+t_1)$ deviates from $\mathbf{R}(t)$ by an angle $\chi(t_1)$ whose mean square is

$$\langle\chi^2(t_1)\rangle=m\langle\chi^2(\tau_c)\rangle\sim 2\alpha(\phi)t_1 . \tag{7.24}$$

From Eq. (7.24) one can see that the Bloch vector loses memory of its initial conditions

$$\mathbf{R}(0)=(0,0,1) \tag{7.25}$$

in a time period of order $[\alpha(\phi)]^{-1}$, when it has rotated by an angle of order unity[44] (see Fig. 14). The criterion (7.23) of the random walk model at the same time justifies application of the decorrelation approximation in solving the Bloch equations (2.10), and leads to the exact solution (5.3) for $\langle\rho_3\rangle$. For $t>[\alpha(\phi)]^{-1}$, the position of the Bloch vector can be regarded as random. For such times, the mean square values of its components are equal, namely

$$\langle\rho_1^2\rangle=\langle\rho_2^2\rangle=\langle\rho_3^2\rangle=\tfrac{1}{3},\quad t>[\alpha(\phi)]^{-1} . \tag{7.26}$$

The second Bloch vector $\tilde{\mathbf{R}}$ has the same initial position (7.25) and undergoes a similar rotation that results in

$$\langle\tilde{\rho}_1^2\rangle=\langle\tilde{\rho}_2^2\rangle=\langle\tilde{\rho}_3^2\rangle=\tfrac{1}{3} \tag{7.27}$$

for times $t>[\alpha(\tilde{\phi})]^{-1}$.

To start the analysis of the relative dephasing of $\mathbf{R}$ and $\tilde{\mathbf{R}}$, we first return to the "absolute" reference frame. Because $\mathbf{H}\neq\tilde{\mathbf{H}}$, the tip of the vector $\tilde{\mathbf{R}}$ follows a trajectory that differs from that of the vector $\mathbf{R}$. To find the relative dephasing of the Bloch vectors induced by fluctuations, one first has to eliminate any possible constant angle θ_0 between their projections on the plane defined by the axes 1 and 2. This angles does not affect the populations ρ_3 and $\tilde{\rho}_3$ and leads only to the constant phase shift between the coherences, $\rho_1+i\rho_2$ and $\tilde{\rho}_1+i\tilde{\rho}_2$, of two atoms. The angle θ_0 is given by

$$\theta_0=\langle\arg\tilde{f}(t)\rangle-\langle\arg f(t)\rangle$$

and can be obtained by the minimization of the expression $\langle|\mathbf{H}-\tilde{\mathbf{H}}_{\theta_0}|^2\rangle$, where $\tilde{\mathbf{H}}_{\theta_0}$ represents the vector $\tilde{\mathbf{H}}$ rotated by the angle θ_0 about the 3 axis. Solving the equation

$$\frac{d}{d\theta_0}\langle|\mathbf{H}-\tilde{\mathbf{H}}_{\theta_0}|^2\rangle=0 \tag{7.28}$$

yields

$$\tan\theta_0=\frac{\alpha_1\sin(\phi-\tilde{\phi})+\alpha_{12}(\sin\phi-\sin\tilde{\phi})}{\alpha_1\cos(\phi-\tilde{\phi})+\alpha_2+\alpha_{12}(\cos\phi-\cos\tilde{\phi})} . \tag{7.29}$$

Only after the Bloch vector $\tilde{\mathbf{R}}$ and its angular velocity vector $\tilde{\mathbf{H}}$ are rotated by the angle θ_0, given by Eq. (7.29), about the 3 axis, which is when the rotations

$$\tilde{\mathbf{R}}\rightarrow\tilde{\mathbf{R}}_{\theta_0};\tilde{\mathbf{H}}\rightarrow\tilde{\mathbf{H}}_{\theta_0}$$

are fulfilled, can one say that the remaining divergence of the trajectories of the Bloch vectors represents the process of their relative dephasing.

We need only consider Bloch vectors $\mathbf{R}$ and $\tilde{\mathbf{R}}_{\theta_0}$ whose tips follow close trajectories, since it is only these atoms for which the relative dephasing is sufficiently small for time $t=t_p$ to contribute appreciably to the signal. In the strong-field regime the necessary condition for a slow relative dephasing of the Bloch vector is

$$\alpha(\phi)\approx\alpha(\tilde{\phi}) . \tag{7.30}$$

Condition (7.30) implies that the two considered atoms are at positions where the intensities of the interference fringes are nearly equal. At time $t\sim[\alpha(\phi)]^{-1}\approx[\alpha(\tilde{\phi})]^{-1}\ll t_p$ when conditions (7.26) and (7.27) are already satisfied, but the relative dephasing is still very small, the correlation function $T(t)$ takes the form

$$T(\alpha^{-1})=\langle\rho_3\tilde{\rho}_3\rangle=\langle\rho_3^2\rangle=\langle\tilde{\rho}_3^2\rangle=\tfrac{1}{3} . \tag{7.31}$$

For $\alpha^{-1}<t\leq t_p$, however, the rotation and, consequently, the process of dephasing of the Bloch vectors continues. As a result, $T(t)$ slowly decreases from $\frac{1}{3}$ and tends towards 0. The question we address is as follows: What is the speed of this process and what is its origin?

By simple geometrical consideration one can show that in the strong-field regime the correlation function $T(t_p)$ is expressed in terms of an internal product of the Bloch vectors $(\mathbf{R}\cdot\tilde{\mathbf{R}})$ as

$$T(t_p)=\tfrac{1}{3}\langle(\mathbf{R}\cdot\tilde{\mathbf{R}})\rangle . \tag{7.32}$$

Equation (7.32) implies that it is convenient to analyze the relative dephasing of the Bloch vectors in a reference frame which we call the "R" frame, tied to the vector $\mathbf{R}$, rather than in the "absolute" frame where both of the vectors are rotating. In the absolute frame each of the three axes of the R frame rotates with the angular velocity $\mathbf{H}$ and at $t=0$ coincides with a corresponding axis of

the absolute frame, that is,

$$\dot{\mathbf{M}}_i=[\mathbf{H}\mathbf{M}_i];\ |\mathbf{M}_i|^2=1\ ,$$
$$m_{ji}(0)=\delta_{ji},\quad j,i=1,2,3\ , \tag{7.33}$$

where the unit vector $\mathbf{M}_i$ with coordinates (m_{1i},m_{2i},m_{3i}) determines direction of the i axis of the R frame at time t. All three vectors $\mathbf{M}_{1,2,3}$ undergo random rotation, remaining perpendicular to each other (see Fig. 14). It has been shown[44] that for $t\gg[\alpha(\phi)]^{-1}$ their coordinates have the following correlations:

$$\langle m_{ji}(t)m_{j'i'}(t-\tau)\rangle=\tfrac{1}{3}\delta_{jj'}\delta_{ii'}\times\begin{cases}e^{-\alpha(\phi)|\tau|} & \text{if } j=1,2\\ e^{-2\alpha(\phi)|\tau|} & \text{if } j=3\ ,\end{cases} \tag{7.34}$$

where the quantity $[\alpha(\phi)]^{-1}$ plays the role of a correlation time.

The vector $\mathbf{R}$ coincides with the 3 axis $\mathbf{M}_3$ of the R frame and, in this frame, is given by $\mathbf{R}_R=(0,0,1)$ at any time, where the script R means that a vector is considered in the R frame. Then, $T(t_p)$ given by Eq. (7.32) transforms into

$$T(t_p)=\tfrac{1}{3}\langle\tilde{\rho}_{R3}\rangle\ , \tag{7.35}$$

where $\langle\tilde{\rho}_{R3}\rangle$ is the average third component of $\tilde{\mathbf{R}}_R$. Thus, the two-atom correlation function in the absolute frame is now expressed in terms of the averaged component of the single Bloch vector in the R frame. Rotation of this vector takes the form

$$\dot{\tilde{\mathbf{R}}}_R=[\delta\mathbf{H}_R\tilde{\mathbf{R}}_R];\delta\mathbf{H}_R=(\tilde{\mathbf{H}}_{\theta_0}-\mathbf{H})_R\ . \tag{7.36}$$

According to Eq. (7.33), the components δh_{Ri} of the vector $\delta\mathbf{H}_R$ are given by

$$\delta h_{Ri}=\sum_{j=1}^{3}m_{ji}(\tilde{\mathbf{H}}_{\theta_0}-\mathbf{H})_j \tag{7.37}$$

and $\delta\mathbf{H}_R$ represents the vector $(\tilde{\mathbf{H}}_{\theta_0}-\mathbf{H})$ that undergoes some additional random rotation. This rotation is inverse to that of the Bloch vector $\mathbf{R}$ in the absolute frame and is described by characteristic time $\sim[\alpha(\phi)]^{-1}$ [see Eq. (7.34)]. All the components of the vector $\delta\mathbf{H}_R$ are fluctuating quantities, and using Eqs. (7.37) and (7.34) one obtains their correlation functions:

$$\langle\delta h_{Ri}(t)\delta h_{Rj}(t-\tau)\rangle=\tfrac{1}{3}\delta_{ij}\{\langle[f(t)-f_{\theta_0}(t)][f^*(t-\tau)-f^*_{\theta_0}(t-\tau)]\rangle+(\delta_-+h_{\mathrm{ad},3}-\tilde{h}_{\mathrm{ad},3})^2e^{-2\alpha(\phi)|\tau|}\},t\gg\alpha(\phi)\ . \tag{7.38}$$

One can see from Eq. (7.38) that fluctuations of the angular velocity vector in the "R" frame are characterized by two correlation times: the time τ_c of the Rabi frequency fluctuations and the time $[2\alpha(\phi)]^{-1}$ associated with random rotation of the component $-(\delta_-+h_{\mathrm{ad},3}-\tilde{h}_{\mathrm{ad},3})_R$ of the vector $\delta\mathbf{H}_R$, the latter time being much larger than τ_c.

Since the dephasing of the Bloch vectors is assumed to be slow relative to their random rotation, $\tilde{\mathbf{R}}_R$ varies only slightly in time $[2\alpha(\phi)]^{-1}$. As $[2\alpha(\phi)]^{-1}$ is the largest correlation time of the fluctuating vector $\delta\mathbf{H}_R$, under this condition the random rotation of the vector $\tilde{\mathbf{R}}_R$ can be considered to be of the random walk character, and the decorrelation approximation can be used in solving Eq. (7.36) [see discussion of Eq. (7.23)]. The third component of the vector $\langle\tilde{\mathbf{R}}_R\rangle$ is then given by

$$\langle\tilde{\rho}_{R3}(t_p)\rangle=e^{-\mu t_p}\ , \tag{7.39}$$

where

$$\mu=2\int_0^\infty\sum_{i=1}^{2}\langle\delta h_{Ri}(t)\delta h_{Ri}(t-\tau)\rangle d\tau\ . \tag{7.40}$$

The speed of dephasing μ can be represented as

$$\mu=\mu_f+\mu_\delta\ , \tag{7.41}$$

where μ_f describes the dephasing induced by fast fluctuations of $\delta\mathbf{H}_R$ (correlation time τ_c), while μ_δ originates from relatively slow fluctuations with correlation time $[2\alpha(\phi)]^{-1}$. Using Eq. (7.38), for μ_f one obtains

$$\mu_f=\tfrac{2}{3}\int_0^\infty\langle[f(t)-f_{\theta_0}(t)][f^*(t-\tau)-f^*_{\theta_0}(t-\tau)]\rangle d\tau\ . \tag{7.42}$$

Carrying out the averaging in Eq. (7.42) and using the expression (7.20) for θ_0 yields

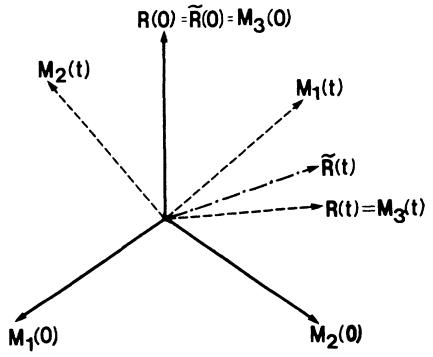

FIG. 14. The positions of the axes $\mathbf{M}_{1,2,3}$ of the "R" frame, tied to the Bloch vector $\mathbf{R}$ ($\mathbf{R}\equiv\mathbf{M}_3$), for time $t=0$ (the solid arrows), and after random rotation, for $t\neq0$ (the dashed arrows). The initial position of the Bloch vector $\tilde{\mathbf{R}}$ coincides with $\mathbf{R}(0)$. However, for time $t\neq0$, owing to difference in angular velocities, $\tilde{\mathbf{R}}(t)$ depicted by the dot-dashed arrow is not equal to $\mathbf{R}(t)$.

$$\mu_f=\frac{2\{2\alpha_1\alpha_2[1-\cos(\phi-\tilde{\phi})]-\alpha_{12}^2(\sin\phi-\sin\tilde{\phi})^2\}}{3[\alpha_1+\alpha_2+\alpha_{12}(\cos\phi+\cos\tilde{\phi})]} . \tag{7.43}$$

The second part of μ,μ_δ, is given by

$$\mu_\delta=\tfrac{2}{3}(\delta_-+h_{\mathrm{ad},3}-\tilde{h}_{\mathrm{ad},3})^2\int_0^\infty e^{-2\alpha(\phi)\tau}d\tau$$
$$=\frac{2[\delta_-+G(t_{12})\alpha_{12}(\sin\phi-\sin\tilde{\phi})]^2}{3[\alpha_1+\alpha_2+\alpha_{12}(\cos\phi+\cos\tilde{\phi})]} , \tag{7.44}$$

where we take into account condition (7.30).

From Eqs. (7.35), (7.39), and (7.41) one finally obtains the correlation function $T(t_p)$ in the form

$$T(t_p)=\tfrac{1}{3}\exp[-(\mu_f+\mu_\delta)t_p] . \tag{7.45}$$

Expression (7.45) coincides with (6.9), since $(\mu_f+\mu_\delta)$ given by Eqs. (7.43) and (7.44) is equal to $-\lambda_1$ given by Eq. (6.10). The part of λ_1 which is independent of δ_- and $G(t_{12})$ coincides with μ_f, while the terms that depend on these parameters are contained in μ_δ.

Since we consider the limiting case where the relative dephasing of the Bloch vectors is a slow process compared with their random rotation, inequality

$$\mu_f,\mu_\delta\ll 2\alpha(\phi)t_p,2\alpha(\tilde{\phi})t_p \tag{7.46}$$

must be satisfied, a condition equivalent to Eq. (C5).

VIII. QUANTITATIVE RESULTS IN A STRONG-RELAXATION LIMIT $\gamma_T T_p \gg 1$

In this section we calculate the PT-3 signal under conditions when relaxation plays an essential role in signal formation. It is assumed that

$$\gamma_t\gg t_p^{-1},(t_{13}-t_{12}-t_p)^{-1}\gg\gamma_l . \tag{8.1}$$

The condition $\gamma_l(t_{13}-t_{12}-t_p)\ll 1$ insures that the signal is not seriously attenuated in a time period between the second and the third pulses. At the same time, the condition $\gamma_t t_p\gg 1$ guarantees that relaxation of atomic coherence plays an essential role during the excitation pulses. The latter condition can result from pressure broadening produced by a buffer gas.

A. Weak-field regime

In a weak-field regime (6.2) and under condition (8.1) the strongest signal is of order $n=\pm 1$. One can use Eq. (2) to obtain the needed Fourier component in the form

$$T^{(1,-1)}(t_p)=\alpha_{12}^2t_p^2+\frac{2\alpha_1\alpha_2\gamma_t t_p}{4\gamma_t^2+\delta_-^2} . \tag{8.2}$$

In the strong-relaxation limit, Eq. (2.23) is no longer valid, and the PT-3 signal must be obtained directly from Eqs. (2.14) and (8.2). Integrating over $\delta_\pm$ in Eq. (2.14), one arrives at the signal

$$W_n^{(3)}=K_0\alpha_{12}^2t_p^2+\frac{K_1\alpha_1\alpha_2t_p}{2\gamma_t} , \tag{8.3}$$

where

$$K_0=\exp\left[\frac{2\gamma_t^2}{\Delta_D^2}\right]\left[1-\mathrm{erf}\left[\frac{\gamma_t\sqrt{2}}{\Delta_D}\right]\right] ,$$
$$K_1=\frac{1}{2}\left[1-\frac{4\gamma_t^2}{\Delta_D^2}\right]K_0+\frac{\gamma_t}{\Delta_D}\sqrt{2/\pi} . \tag{8.4}$$

Similar to the signal in the weak-relaxation limit [see Eq. (6.7)], the signal (8.3) does not depend on the delay time. However, in contrast to that case, the first term in Eq. (8.3), which depends on the correlation of the pulses and is proportional to the square of the mean amplitude $\rho^{(1)}(t_p)$ of the population difference grating, can be much larger than the second term proportional to $\alpha_1\alpha_2$, which is independent of this correlation and originates from the stochastic part of the grating.

B. Moderate and strong-field regimes

If the intensity of the pulses increases so that $\alpha_{\max}t_p\geq 1$, the correlation function $T(t_p)$ is given by

$$T(t_p)=e^{-2xt_p}\left[1+\frac{8|Q|^2\gamma_t t_p}{4\gamma_t^2+\delta_-^2}\right]+T_0 , \tag{8.5}$$

where x and Q are defined in Eqs. (4.5) and (4.6) and we neglect all the terms leading to minor contributions to the PT-3 signal. Using Eqs. (2.19), (2.14), and (8.5) one obtains the PT-3 signal

$$W_n^{(3)}=e^{-2(\alpha_1+\alpha_2)t_p}\left[K_0I_n^2(\zeta)+\frac{K_1t_p}{2\gamma_t}\{\alpha_1\alpha_2[I_{n+1}^2(\zeta)+I_{n-1}^2(\zeta)]+(\alpha_1^2+\alpha_2^2+2\alpha_{12}^2)I_n^2(\zeta)\right.$$
$$\left.+2\alpha_{12}^2I_{n-1}(\zeta)I_{n+1}(\zeta)-2\alpha_{12}(\alpha_1+\alpha_2)I_n(\zeta)[I_{n-1}(\zeta)+I_{n+1}(\zeta)]\}\right]+O\left[\frac{\gamma_l^2}{\alpha_{\max}\gamma_t}\right] , \tag{8.6}$$

where I_n is a modified Bessel function and $\zeta=2\alpha_{12}t_p$. The last term in Eq. (8.6), proportional to γ_l^2, is contributed by the steady-state solution T_0, and should be taken into account only when the rest of the signal vanishes.

When the intensity of the pulses increases, so that a strong-field regime (6.8) is realized, two very different situations may occur, depending on the degree of the mutual correlation of the pulses and their intensities.

If the pulses are almost fully correlated and have almost equal intensities ($\alpha_1\approx\alpha_2\approx\alpha_{12}=\alpha$), so that condition (6.52) is satisfied, the first term in Eq. (8.6) dominates, and the PT-3 signal is given by

$$W_n^{(3)}=K_0\frac{\exp(-n^2/2\alpha t_p)}{4\pi\alpha t_p}e^{-2(\alpha_1+\alpha_2-2\alpha_{12})t_p} . \quad (8.7)$$

The signal (8.7) does not exhibit any dependence on delay time t_{12} and for $n\ll\sqrt{\alpha t_p}$ it represents a plateau of height $(4\pi\alpha t_p)^{-1}$, provided $\alpha t_{12}\ll 1$. The PT-3 signal (8.7) is completely determined by the mean amplitude of the population grating, since

$$W_n^{(3)}=K_0\rho^2(n) . \quad (8.8)$$

In contrast with the results in a weak-relaxation limit (see discussion at the end of Sec. VI), when $\gamma_t t_p\gg 1$, the stochastic contribution to the population grating is effectively suppressed, while the mean amplitude is not effected by the relaxation of atomic coherence. Transition from the weak-relaxation limit to the strong-relaxation one is shown in Fig. 15.

For noncorrelated pulses or correlated pulses with very different intensities, condition

$$\alpha_1+\alpha_2\gg 2\alpha_{12},t_p^{-1} \quad (8.9)$$

is satisfied, and the terms which are proportional to K_0 and K_1 in Eq. (8.6) become exponentially small. In the limit (8.9), which we examine for the remainder of this section, the signal is solely determined by the contribution from the steady-state solution T_0.

For moderate field intensities

$$t_p^{-1}\ll\alpha_{\max}\ll\gamma_t \quad (8.10)$$

one can approximate

$$T(t_p)\approx T_0=\frac{\gamma_l^2}{(\alpha_1+\alpha_2)^2}\left[1-\frac{2\alpha_{12}}{\alpha_1+\alpha_2}(\cos\phi+\cos\tilde{\phi})+\frac{4\alpha_{12}^2}{(\alpha_1+\alpha_2)^2}\cos\phi\cos\tilde{\phi}+\frac{8|Q|^2\gamma_t}{(\alpha_1+\alpha_2)(4\gamma_t^2+\delta_-^2)}\right] . \quad (8.11)$$

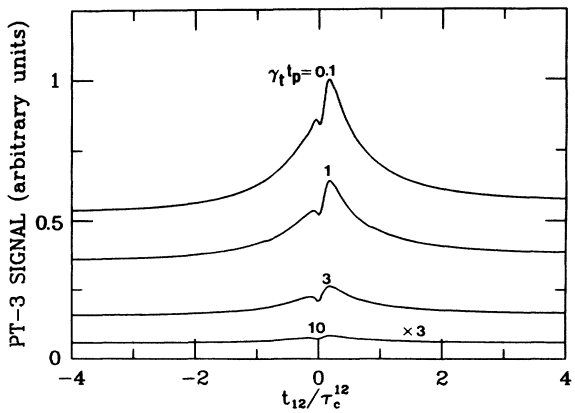

FIG. 15. Signals of order $n=1$ vs t_{12}/τ_c^{12} for different transverse relaxation parameter $\gamma_t t_p$ in the case of weak longitudinal relaxation: $\gamma_l t_p=0.2$. The fully correlated ($\Phi=1$) pulses have nearly equal intensities $\alpha_1 t_p=100$, $\alpha_2 t_p=105$, and $\Delta_D t_p=14$.

The strongest signal occurs for orders $n=\pm 1$. Picking up the terms proportional to $\exp[i(\phi-\tilde{\phi})]$ and integrating over $\delta_\pm$ in Eq. (2.14), one finds the PT-3 signal

$$W_{\pm 1}^{(3)}=\frac{\gamma_l^2}{(\alpha_1+\alpha_2)^2}\left[\frac{K_0\alpha_{12}^2}{(\alpha_1+\alpha_2)^2}+\frac{2K_1\alpha_1\alpha_2}{(\alpha_1+\alpha_2)\gamma_t}\right] , \quad (8.12)$$

which exhibits no dependence on delay time.

However, when the pulses become very strong,

$$\alpha_1+\alpha_2\gg\alpha_{12},\gamma_1 , \quad (8.13)$$

one has

$$T(t_p)=T_0=\frac{\gamma_l^2}{y+\delta_f^2+x\gamma_t} . \quad (8.14)$$

It is shown below that in the regime (8.13), which can be interpreted as a strong-field regime in a strong-relaxation limit, the correlation function (8.14) leads to the PT-3 signal whose dependence on delay time resembles very much that in a strong-field regime in a weak-relaxation limit. Integrating over ϕ_- in Eq. (2.19) and over $\delta_\pm$ in Eq. (2.14) yields

$$W_n^{(3)}=\frac{2K_0\gamma_l^2}{\pi\gamma_t(\alpha_1+\alpha_2)}\times\int_0^{\pi/2}\frac{\{1+Y^{-1}-[(1+Y^{-1})^2-1]^{1/2}\}^n}{\sqrt{1+2Y}}d\phi_+ , \quad (8.15)$$

where

$$Y=2\eta_\gamma^2[1-\Phi(1-G^2)\cos^2\phi_+] ,$$
$$\eta_\gamma=\left[\frac{\alpha_1\alpha_2}{(\alpha_1+\alpha_2)\gamma_t}\right]^{1/2} . \quad (8.16)$$

For one strong and one weak pulse,

$$\alpha_{\min}\ll\gamma_t\ll\alpha_{\max} ,$$

it follows that $Y\ll 1$ in Eq. (8.15), so that the signal can be approximated as

$$W_n^{(3)}=\frac{2K_0\gamma_l^2\alpha_{\min}}{\gamma_t^2\alpha_{\max}}[2-\Phi(1-G^2)] . \quad (8.17)$$

The signal (8.17) has the same dependence on the correlation and delay times as the weak-relaxation limit signal (6.14), but it is much weaker.

If both pulses are strong, that is if

$$\alpha_1,\alpha_2\gg\gamma_t , \quad (8.18)$$

the main contribution to the integral in Eq. (8.15) comes from the regions where $Y\gg 1$, and for $n\neq 0$, Eq. (8.15) can be transformed into

$$W_n^{(3)}=\frac{2K_0\gamma_l^2}{\pi\gamma_t(\alpha_1+\alpha_2)}\int_0^{\pi/2}\frac{\exp(-n\sqrt{2}/\sqrt{Y})}{\sqrt{2Y}}d\phi_+ . \quad (8.19)$$

The integral in Eq. (8.19) can be estimated by the same

method used to approximate the integral in Eq. (D7). The strongest signal, characterized by small n, $n \ll \eta_\gamma$, for strongly correlated pulses $(1-\Phi \ll 1)$ exhibits a symmetrical peak centered at $t_{12}=0$. The signal intensity for $t_{12} \leq \tau_c^{12}$ is given by

$$W_n^{(3)} = \frac{K_0 \gamma_l^2}{\pi(\alpha_1+\alpha_2)\gamma_t \eta_\gamma} \times \ln \frac{2\eta_\gamma}{n[\exp(-Z/2)+\sqrt{Z+\exp(-Z)}]} , \quad (8.20)$$

where

$$Z = \frac{[1-\Phi(1-G^2)]\eta_\gamma^2}{n^2} . \quad (8.21)$$

If one compares Eqs. (8.20) and (6.29), one finds that the signals in the strong-relaxation and in the weak-relaxation limits are similar, if $\alpha_{\max} \gg \alpha_{\min}$ (see Fig. 16). The peak has width $|t_{12}| \approx \tau_c^{12}$ and for fully correlated pulses ($\Phi=1$), is approximately $\ln(\eta_\gamma/n)$ times higher than the background signal

$$W_n^{(3)} = \frac{K_0 \gamma_l^2}{\pi(\alpha_1+\alpha_2)\gamma_t \eta_\gamma} , \quad (8.22)$$

which would be obtained for non-correlated pulses ($\Phi=0$).

The signal of higher order $n > \eta_\gamma \gg 1$, is given by

$$W_n^{(3)} = \frac{2K_0 \gamma_l^2}{\pi(\alpha_1+\alpha_2)\gamma_t \eta_\gamma} \exp\left[-\frac{n[4+\Phi(1-G^2)]}{4\eta_\gamma}\right] \times I_0\left[\frac{n\Phi(1-G^2)}{4\eta_\gamma}\right] . \quad (8.23)$$

For fully correlated pulses the signal (8.23) exhibits a profound dip centered at $t_{12}=0$, and for $|t_{12}| > \tau_c^{12}$ it coincides with the signal for noncorrelated pulses.

One can see from the results presented above, that under condition (8.13) the PT-3 signal in the strong-relaxation regime resembles that in the weak-relaxation time, attenuated approximately by a factor

$$\frac{3\sqrt{2\pi}K_0\gamma_l^2}{2\gamma_t(\alpha_1+\alpha_2)} \ll 1 ; \quad (8.24)$$

while the parameter $3(4\gamma_t)^{-1}$ plays the role of the effective pulse duration.

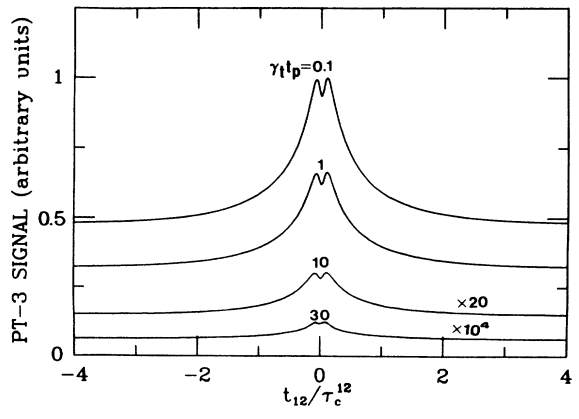

FIG. 16. Signals of order $n=1$ vs t_{12}/τ_c^{12} for different transverse relaxation parameter $\gamma_t t_p$ and a small longitudinal relaxation parameter: $\gamma_l t_p=0.2$. The fully correlated ($\Phi=1$) pulses have very different intensities $\alpha_1 t_p=100$, $\alpha_2 t_p=10^4$, and $\Delta_D t_p=14$.

IX. SUMMARY AND DISCUSSION

In this paper we have considered pulses with rectangular envelopes; that is, rise and fall times t_r and t_f of the pulses have been assumed to be negligible:

$$t_r=t_f=0 . \quad (9.1)$$

If one takes into account nonzero values of t_r and t_f, one sees that, for the symmetrical part of the signal, W_S, generalization of the results obtained in Sec. VI is straightforward. Since W_S is proportional to $T^{(n,-n)}(t_p,\delta,\delta)$, one can show that all the results for W_S remain valid provided that the substitution

$$\alpha_{ii} t_p \Longrightarrow \int_{-\infty}^{+\infty} \alpha_{ii}(t)dt \quad (9.2)$$

is made. Thus, the results leading to nearly symmetrical signals can be still used. However, the asymmetrical part of the signal may undergo serious charge, if $t_r, t_f > \alpha^{-1}, \Delta_D^{-1}$. In this case the effective range of detunings that can contribute to the signal narrows from Δ_D to $\min(t_r^{-1}, t_f^{-1})$. As a result, the parameter D increases:

$$D = \frac{3(\alpha_1+\alpha_2)}{4\Delta_D^2 t_p} \Longrightarrow D \sim \frac{(\alpha_1+\alpha_2)\max(t_r^2,t_f^2)}{t_p} , \quad (9.3)$$

and asymmetry of the signal up to order $n=\alpha \max(t_r,t_f)$ is suppressed [see Eqs. (36) and (38)]. If $\max(t_r,t_f) \sim t_p$, signals of all orders become symmetrical.

It has been shown in Sec. VI that in a weak-relaxation limit the PT-3 signal in many cases depends only weakly on correlation properties of the pulses when $|t_{12}| > \tau_c^{12}$. This effect, however, cannot be interpreted as a loss of memory of the pulse correlations by the two-level atoms. This memory is preserved, if $\alpha|t_{12}| \ll 1$, and can be revealed under certain conditions, as in the case of the signals of high orders induced by excitation pulses having equal intensities. The origin of the Φ independence of the PT-3 signal for $|t_{12}| > \tau_c^{12}$ can be related to the fact that the third pulse is weak and noncorrelated with the first two. As a result, in the weak-relaxation and the strong-field limit, different velocity groups of atoms contribute to the signal independently [$W_n^{(3)} \approx T(t_p,\delta,\delta)$]. It will be shown elsewhere that in the case of two-pulse transients, when the atoms with different velocities might contribute to the signal coherently, the difference in the signals for correlated and noncorrelated pulses for $|t_{12}| > \tau_c^{12}$ can be significant.

In summary, we have studied the three-pulse optical coherent transients induced by broad-bandwidth pulses. Within the approximation of a small delay time between

the first two excitation pulses, we have considered, analytically and numerically, different values for the pulse intensities, relaxation times, and Doppler width. It was shown that if the intensities of the excitation pulses are high enough, stochastic spatial gratings of many orders can be created in the population difference of two-level atoms and the signals with comparable energies might be emitted in many directions. These signals, as functions of the delay time, can vary significantly on the time scale of the cross-correlation time τ_c^{12} of the pulses, provided the relaxation processes in the atomic vapor are negligible on this time scale. We predict that the signal for order $n \ll (\alpha_{\min} t_p)^{1/2}$ as a function of delay time exhibits a peak having width $|t_{12}| \sim \tau_c^{12}$. When the pulses are strongly correlated and their intensities are not equal, this peak has a very narrow dip at $t_{12}=0$ whose width is much smaller than τ_c^{12}. The signals of higher order can exhibit either a dip or a considerable negative asymmetry depending on the Doppler width of the atomic ensemble and ratio of intensities of the excitation pulses. All these features occur for strongly correlated pulses, when $\alpha_{\min} t_p > 1$.

For a two-level atom driven by two arbitrary pulses with delay time t_{12} satisfying $|t_{12}| \ll \alpha_{\max}$, we have shown that the final position of its Bloch vector can be described as a result of rotation performed under the influence of two fully overlapping pulses that coincide with the original pulses. However, as a result of this transformation, an additional fluctuating detuning parameter appears in the Bloch equations, which is the only effect of the time delay of the pulses. We have interpreted the obtained results by using this model.

If the relaxation cannot be neglected and the signal is detectable ($T_2 < t_p < T_1$), the signal, induced by fully correlated pulses with equal intensities, is much stronger than in all other cases and does not show any dependence on delay time. If the intensities are different, the PT-3 signal exhibits a profile which resembles that in a weak-relaxation regime; however, the signal is much weaker.

The experiments performed on different atomic vapors indicate that the PT-3 signal is very sensitive to the atomic level structure, which is usually much more complicated than a two-level system. The only experiment,[15] of which we are aware, where the active atoms could be realistically approximated as a two-level system, revealed direct dependence of the signal on τ_c^{12} in the case when one of the pulses was strong. Extension of this work to the case of two strong pulses would allow for a more complete test of our results.

ACKNOWLEDGMENTS

We would like to thank J.-L. Le Gouët and J.-C. Keller for many useful discussions. This research is supported by the U.S. Office of Naval Research and the National Science Foundation under Grant No. INT88015036.

APPENDIX A: GENERAL EXPRESSION FOR THE PT-3 SIGNAL

The energy $\mathcal{W}_n^{(3)}$ of the PT-3 signal radiated in the direction $\mathbf{k}_3 + n\mathbf{k}_d$ under the influence of the third pulse that starts at time t_3, $t_3 = t_{12} + t_{23}$, and has duration t_{3p} can be defined as[12]

$$\mathcal{W}_n^{(3)} = C(\Delta_D^2 \pi)^{-1} \int\int \psi(\delta - \Delta)\psi(\tilde{\delta} - \Delta) \left[\int_{t_3}^{\infty} \langle \rho_{ab}^{(n)}(t;\delta) \rho_{ab}^{(-n)}(t;\tilde{\delta}) \rangle dt \right] d\delta \, d\tilde{\delta} \ , \tag{A1}$$

where C is a constant. The third pulse is weak, and therefore a component $\rho_{ab}^{(n)}$ of the atomic coherence ρ_{ab} satisfies the equation

$$\dot{\rho}_{ab}^{(n)} = -(\gamma_t + i\delta)\rho_{ab}^{(n)} + i f_3 \rho_3^{(n)}(t_p^0) e^{-\gamma_l (t - t_p^0)} \ , \tag{A2}$$

where

$$\rho_{ab}(\mathbf{r}) = \sum_n \rho_{ab}^{(n)} e^{i(\mathbf{k}_3 + n\mathbf{k}_d)r}, \quad f_3 = \mu_{ab} \hbar^{-1} \mathcal{E}_3(t) \ . \tag{A3}$$

Substituting the solution of Eq. (A2) into Eq. (A1), one has

$$\begin{aligned} \mathcal{W}_n^{(3)} = C(\Delta_D^2 \pi)^{-1} \int\int \psi(\delta - \Delta)\psi(\tilde{\delta} - \Delta) \\ \times \left[\int_0^{\infty} dt \int_0^t dt' \int_0^t dt'' \langle f_3(t' + t_3) f_3^*(t'' + t_3) \right. \\ \times e^{-\gamma_l (t_{13} - t_p^0 + t' + t'') - (i\delta + \gamma_t)(t - t') - (-i\tilde{\delta} + \gamma_t)(t - t'')} \\ \left. \times \rho_3^{(n)}(t_p^0;\delta) \rho_3^{(-n)}(t_p^0;\tilde{\delta}) \rangle \right] d\delta \, d\tilde{\delta} \ . \end{aligned} \tag{A4}$$

Since the third pulse is not correlated with the first two excitation pulses, averaging in Eq. (A4) can be carried out separately for $f_3(t' + t_3) f_3^*(t'' + t_3)$ and $\rho_3^{(n)}(t_p^0;\delta)\rho_3^{(-n)}(t_p^0;\tilde{\delta})$. Using the approximation of δ-correlated fluctuations for the third pulse,

$$\langle f_3(t' + t_3) f_3^*(t'' + t_3) \rangle = \alpha_3 \delta(t' - t'') \ , \tag{A5}$$

where $0<t',t''<t_{3p}$, and $\alpha_3=\langle|f_3|^2\rangle\tau_c^{33}$, and integrating over t'', t, and t' in Eq. (A4), one finally gets the expression

$$\mathcal{W}_n^{(3)}=C(2\gamma_l\Delta_D^2\pi)^{-1}\alpha_3(1-e^{-2\gamma_l t_{3p}})e^{-2\gamma_l(t_{13}-t_p^0)}\int\int\frac{\psi(\delta-\Delta)\psi(\tilde{\delta}-\Delta)}{2\gamma_t+i\delta_-}\langle T_{33}^{(n,-n)}(t_p^0;\delta,\tilde{\delta})\rangle d\delta\, d\tilde{\delta}\ . \tag{A6}$$

Introducing $W_n^{(3)}$ by the relation

$$W_n^{(3)}=[C\sqrt{\pi}\alpha_3(1-e^{-2\gamma_l t_{3p}})]^{-1}2\gamma_l\Delta_D e^{2\gamma_l(t_{13}-t_p^0)}\mathcal{W}_n^{(3)}\ , \tag{A7}$$

one obtains Eq. (2.14).

APPENDIX B: EXPRESSION FOR $T^{(1,-1)}(t)$ IN A WEAK-FIELD REGIME

In a weak-field regime

$$\alpha_1,\alpha_2\ll\max[t_p^{-1},\min(\gamma_l,\gamma_t)] \tag{B1}$$

perturbation theory can be applied in Eqs. (4.1)–(4.3). This is more convenient than taking the weak-field limit of the general solution (5.4). The population gratings of order ±1 dominate the process and lead to the signals of equal intensity. Iterating Eqs. (4.1)–(4.3) twice yields

$$T(t;1,-1)=\frac{\alpha_{12}^2}{\gamma_l^2}(1-e^{-\gamma_l t})^2+2\alpha_1\alpha_2\int_0^t\int_0^{t'}e^{-2\gamma_l(t-t')-2\gamma_t(t'-t'')}\times\cos\delta_-(t'-t'')dt'dt''\ . \tag{B2}$$

In a weak-relaxation limit (6.1), one obtains Eq. (6.3). In the case of strong transverse relaxation (8.1), Eq. (B2) leads to Eq. (8.2).

APPENDIX C: EXPRESSION FOR $T(t_P)$ IN A WEAK-RELAXATION LIMIT IN A STRONG-FIELD REGIME

In a weak-relaxation limit (6.1) the solution (5.4) is given by

$$T(t_p)=\sum_{i=1}^{3}e^{\lambda_i t_p}T_i\ , \tag{C1}$$

where the exponents $\lambda_{1,2,3}$ are the roots of the equation

$$\lambda(\lambda+x)(\lambda+3x)=-2y(\lambda+x)-\delta_f^2(\lambda+2x)\ . \tag{C2}$$

At time t_p, only those atoms whose Bloch vectors have not dephased contribute to the signal. In the weak-relaxation limit, the main contributions to the integral (2.19) come from those regions $(\phi,\tilde{\phi})$, where solution (C1) is not exponentially small, that is, where at least one of the indexes λ_i satisfies the condition

$$\lambda_i t_p\ll1\ . \tag{C3}$$

If the pulses are not fully correlated or their intensities are not very close to each other, i.e., if

$$(\alpha_1+\alpha_2-2\alpha_{12})t_p\gg1\ , \tag{C4}$$

the regions in the plane $(\phi,\tilde{\phi})$ that satisfy requirement (C3) are defined by condition

$$\sqrt{y},\delta_f\ll x\ . \tag{C5}$$

Then the roots of Eq. (C2) are given by

$$\lambda_1=-\frac{2(y+\delta_f^2)}{3x}\ ,\qquad \lambda_2\approx-x,\quad \lambda_3\approx-3x \tag{C6}$$

with $T_{1,2,3}$ being being equal to

$$T_1\approx\tfrac{1}{3},|T_2|\ll1,T_3\approx\tfrac{2}{3}\ . \tag{C7}$$

The root λ_1 is much smaller than the other two; under condition (C4) it follows that $xt_p\gg1$, and only the term having index λ_1 on the right-hand side of Eq. (C1) can provide a contribution which is not exponentially small. Taking into account Eqs. (C6) and (C7) yields

$$T(t_p)=\tfrac{1}{3}\exp\left[-\frac{2(y+\delta_f^2)t_p}{3x}\right]\ . \tag{C8}$$

If condition (C5) is violated, the difference between the exact solution (C1) and the approximate solution $T(t_p)$ given by Eq. (C8) is exponentially small. Thus, one can use Eq. (C8) for any y, δ_f, and x.

If the pulses are fully correlated and have almost equal intensities, i.e.,

$$(\alpha_1+\alpha_2-2\alpha_{12})t_p<1\ , \tag{C9}$$

condition (C5) is violated for the atoms situated close to the minima of the interference fringes, the regions for which the field is weak. Consequently, for

$$|\phi\pm\pi|,|\tilde{\phi}\pm\pi|\ll\frac{1}{[(\alpha_1+\alpha_2)t_p]^{1/2}}\ll1\ . \tag{C10}$$

Equation (C8) is not valid. Despite this fact we are still be able to use Eq. (C8) since the contribution to the PT-3 signal from these regions is of order of $[(\alpha_1+\alpha_2)t_p]^{-1}$ and can be neglected.

Hence we may conclude that in a strong-field regime the signal is governed by the term (C8) alone. Taking into account expressions (4.5), (4.7), and (5.7), one gets Eqs. (6.9)–(6.10) of the text.

APPENDIX D: CALCULATION OF $W_N^{(3)}$ IN A STRONG-FIELD REGIME

Using the symmetry of Eq. (6.10) under the permutations

$$\phi \leftrightarrow -\tilde{\phi}+2\pi m\,;\ m=0,\pm 1,\ldots$$

we can rewrite Eq. (2.19) as

$$T^{(n,-n)}(t_p;\delta_-)=\frac{1}{\pi^2}\int_0^{\pi}d\phi_+\int_{-\pi/2}^{\pi/2}T(t_p)e^{-2in\phi_-}d\phi_-\ , \tag{D1}$$

with

$$T(t_p;\delta_-)=\tfrac{1}{3}\exp[-2t_p(4\sin^2\phi_-\{\alpha_1\alpha_2-[1-G^2(t_{12})]\alpha_{12}^2\cos^2\phi_+\}$$
$$+\delta_-^2+4\delta_- G(t_{12})\alpha_{12}\sin\phi_-\cos\phi_+)[3(\alpha_1+\alpha_2+2\alpha_{12}\cos\phi_-\cos\phi_+)]^{-1}]\ . \tag{D2}$$

In order to obtain the analytical expressions for the PT-3 signal with two strong pulses, one substitutes (D1) in Eq. (2.23) and carries out the δ_- integration to obtain

$$W_n^{(3)}=W_S+W_{AS}\ , \tag{D3}$$

with symmetrical, W_S, and asymmetrical, W_{AS}, parts of the signal given by

$$W_S=\frac{2}{3\pi^2}\int_0^{\pi}d\phi_+\int_0^{\pi/2}d\phi_-e^{-b}\cos 2n\phi_-\ , \tag{D4}$$

$$W_{AS}=\frac{2i}{3\pi^2}\int_0^{\pi}d\phi_+\int_0^{\pi/2}d\phi_-e^{-b}\sin(2n\phi_-)\mathrm{erf}(ia)\ , \tag{D5}$$

where erf is an error function and

$$a=\frac{\sqrt{2\Phi}G\eta\sin\phi_-\cos\phi_+}{\{(1+\sqrt{\Phi}\beta\cos\phi_-\cos\phi_+)[1+D(1+\sqrt{\Phi}\beta\cos\phi_-\cos\phi_+)]\}^{0.5}}\ ,$$
$$b=\frac{2\eta^2\sin^2\phi_-(1-\Phi_0\cos^2\phi_-)}{1+\sqrt{\Phi}\beta\cos\phi_-\cos\phi_+}\ , \tag{D6}$$
$$\eta=\left[\frac{4\alpha_1\alpha_2 t_p}{3(\alpha_1+\alpha_2)}\right]^{1/2}\gg 1,\quad \Phi_0=\Phi(1-G^2)\le 1,\quad \beta=\frac{2(\alpha_1\alpha_2)^{1/2}}{\alpha_1+\alpha_2}\le 1,\quad D=\frac{3(\alpha_1+\alpha_2)}{4\Delta_D^2 t_p}\ .$$

Using the fact that $\eta\gg 1$, one can analytically carry out the ϕ_- integration in Eq. (D4) provided $n\neq 0$. Using these conditions, the approximation $\sin\phi_-\approx\phi_-,\cos\phi_-\approx 1$ in expressions (D6) for a and b, and setting the upper integration limit equal to ∞, we carry out the integration over ϕ_- in Eq. (D4) to obtain

$$W_S=\frac{1}{3\eta\pi\sqrt{2\pi}}\int_0^{\infty}\left[\frac{1+\sqrt{\Phi}\beta\cos\phi_+}{1-\Phi_0\cos^2\phi_+}\right]^{1/2}\exp\left[-\frac{n^2(1+\sqrt{\Phi}\beta\cos\phi_+)}{2\eta^2(1-\Phi_0\cos^2\phi_+)}\right]d\phi_+\ . \tag{D7}$$

If, in addition, the inequality

$$(1-\Phi_0)\eta^2>1 \tag{D8}$$

is satisfied, it is also possible to carry out similar integration in Eq. (D5) that yields

$$W_{AS}=\frac{1}{3\eta\pi\sqrt{2\pi}}\int_0^{\pi}\left[\frac{1+\sqrt{\Phi}\beta\cos\phi_+}{1-\Phi_0\cos^2\phi_+}\right]^{1/2}\exp\left[-\frac{n^2(1+\sqrt{\Phi}\beta\cos\phi_+)}{2\eta^2(1-\Phi_0\cos^2\phi_+)}\right]\mathrm{erf}(\chi)d\phi_+\ , \tag{D9}$$

where

$$\chi=\frac{Gn\sqrt{\Phi}\cos\phi_+}{\sqrt{2}\eta(1-\Phi_0\cos^2\phi_+)}\left[D+\frac{(1-\Phi\cos^2\phi_+)}{(1-\Phi_0\cos^2\phi_+)(1+\sqrt{\Phi}\beta\cos\phi_+)}\right]^{-0.5}\ . \tag{D10}$$

1. Weak mutual correlation of the pulses

Assuming that

$$\frac{\Phi}{4}\left[1+\frac{n^2}{\eta^2}\left[1+\frac{n^2}{(\alpha_1+\alpha_2)t_p}\right]\right]\ll 1\ , \tag{D11}$$

it follows that

$$\beta,\Phi_0 \ll \left[1+\frac{n^2}{\eta^2}\right]^{-1};\chi \ll 1 ,$$

and that inequality (D8) is valid. Extracting the terms of zero, first, and second orders in $\sqrt{\Phi}$ in the integrals (D7) and (D9) one finds

$$W_n^{(3)}=\frac{e^{-n^2/2\eta^2}}{3\eta\pi\sqrt{2\pi}}\int_0^{\pi}\left\{1+\sqrt{\Phi}\cos\phi_+\left[\frac{\beta}{2}\left[1-\frac{n^2}{\eta^2}\right]+\frac{Gn}{\eta\sqrt{D+2}}\right]\right.$$
$$\left.+\cos^2\phi_+\left[\frac{\Phi_0}{2}\left[1-\frac{n^2}{\eta^2}\right]-\frac{\Phi\beta^2}{8}\left[1+\frac{2n^2}{\eta^2}-\frac{n^4}{\eta^4}\right]+\frac{\Phi\beta Gn}{\eta\sqrt{2\pi(1+D)}}\left[\frac{2+D}{1+D}-\frac{n^2}{\eta^2}\right]\right]\right\}d\phi_+ . \tag{D12}$$

Carrying out the integration in (D12), one recovers Eq. (6.19).

2. Strongly correlated pulses

In this case $1-\Phi \ll 1$, and $(1-\Phi)$ is treated as a small parameter. The remainder of this Appendix is devoted to a consideration of this limit.

a. Signals of order $n \ll \eta$. First we consider signals, characterized by small n, $n \ll \eta$. To estimate the symmetrical part of the signal, W_S, from Eq. (D7), we observe that the expression under the integral sign is not exponentially small only if $y_+ \le \phi_+ \le \pi - y_-$, where $y_\pm$ can be expressed as

$$y_\pm=\frac{n\sqrt{1\pm\beta\sqrt{\Phi}}}{\eta}\exp\left[-\frac{(1-\Phi_0)\eta^2}{(1\pm\beta\sqrt{\Phi})n^2}\right]\ll 1 . \tag{D13}$$

Taking into account only the contributions which are not exponentially small, one has

$$W_S=\frac{1}{3\eta\pi\sqrt{2\pi}}\left[\int_0^{\pi}\left[\frac{1+\sqrt{\Phi}\beta\cos\phi_+}{1-\Phi_0\cos^2\phi_+}\right]^{1/2}d\phi_+-\int_0^{y_+}\left[\frac{1+\sqrt{\Phi}\beta}{1-\Phi_0(1-\phi_+^2)}\right]^{1/2}d\phi_+\right.$$
$$\left.-\int_0^{y_-}\left[\frac{1-\sqrt{\Phi}\beta}{1-\Phi_0(1-\phi_+^2)}\right]^{1/2}d\phi_+\right] . \tag{D14}$$

Expanding $(1+\beta\sqrt{\Phi}\cos\phi_+)^{1/2}$ in terms of $\beta\sqrt{\Phi}$ up to the fifth order in the first term of Eq. (D14) gives good accuracy even for $\beta=1$. In this limit the integrals reduce to

$$W_S=\frac{1}{3\eta\pi\sqrt{2\pi}}\left\{\left[2-\frac{\Phi\beta^2}{4\Phi_0}-\frac{5(2+\Phi_0)\Phi^2\beta^4}{192\Phi_0^2}\right]F(\Phi_0)+\frac{\Phi\beta^2}{4\Phi_0}\left[1+\frac{5(1+\Phi_0)\Phi\beta^2}{96\Phi_0}\right]E(\Phi_0)\right.$$
$$\left.-\sum_{\pm}\left[\frac{1\pm\sqrt{\Phi}\beta}{\Phi_0}\right]^{1/2}\ln\left[\frac{(\Phi_0)^{1/2}y_\pm}{(1-\Phi_0)^{1/2}}+\left[1+\frac{\Phi_0 y_\pm^2}{1-\Phi_0}\right]^{1/2}\right]\right\} , \tag{D15}$$

where F and E are elliptic integrals of the first and second kind,[43] respectively.

Under the assumption that $(1-\Phi_0)\ll 1$, one can use asymptotic expressions for the elliptical functions, and, taking into account the fact that

$$2-\frac{\Phi\beta^2}{4\Phi_0}-\frac{5(2+\Phi_0)\Phi^2\beta^4}{192\Phi_0^2}\approx(1+\sqrt{\Phi}\beta)^{1/2}+(1-\sqrt{\Phi}\beta)^{1/2} , \tag{D16}$$

one can arrive at Eq. (6.30) of the text.

For $t_{12}\gg\tau_c^{12}$ it follows that $G=1$ and $\Phi_0=0$, and thus $y_\pm=0$. Although the accuracy of Eq. (D15) is reasonably good, one can use the more accurate expression (D14) to obtain the background value of W_S:

$$W_S(t_{12}\gg\tau_c)=\frac{\sqrt{2}}{3\pi\eta\sqrt{\pi}}\left[1+\frac{2\alpha_{12}}{\alpha_1+\alpha_2}\right]^{1/2}E\left[\frac{4\alpha_{12}}{\alpha_1+\alpha_2+2\alpha_{12}}\right] . \tag{D17}$$

The background signal depends only weakly on the correlation parameter Φ, and, independent of Φ, differs by at most 10% from the value

$$W_n^{(3)}=\frac{1}{3\eta\sqrt{2\pi}} ,$$

which would be obtained for noncorrelated pulses ($\Phi=0$). For $\alpha_{\min}\ll\alpha_{\max}$ one obtains Eq. (6.37), while for $\alpha_1=\alpha_2;\Phi=1$, Eq. (D17) leads to the symmetrical part of Eq. (6.42).

To estimate the asymmetrical part of the signal, W_{AS}, we represent it in the form

$$W_{AS}=A_+-A_- , \tag{D18}$$

where, according to Eq. (D5), $A_\pm$ is given by

$$A_\pm=\frac{2i}{3\pi^2}\int_0^{\pi/2}d\phi_+\int_0^{\pi/2}d\phi_- e^{-b_\pm}\sin(2n\phi_-)\mathrm{erf}(ia_\pm) , \tag{D19}$$

and $a_\pm=a(\pm\beta),b_\pm=b(\pm\beta)$. It is not difficult to show that $A_\pm>0$, and thus the signal has a positive asymmetry, when $A_+>A_-$, and a negative one in the opposite case.

If $(1-\Phi_0)\eta<1$, one has to evaluate this exact expression. However, if $(1-\Phi_0)\eta>1$, one can use Eq. (D9) to approximate it as

$$A_\pm=\frac{1}{3\eta\pi\sqrt{2\pi}}\int_{y_\pm}^{\pi/2}\left[\frac{1\pm\sqrt{\Phi}\beta\cos\phi_+}{1-\Phi_0\cos^2\phi_+}\right]^{1/2}\mathrm{erf}(\chi_\pm)d\phi_+ , \tag{D20}$$

where $\chi_\pm=\chi(\pm\beta)$.

In the case of small order $n,n\ll\eta$, which is considered now, it is shown below that $W_{AS}<W_S$; however, there are certain cases where W_{AS} qualitatively modifies the signal. Such a modification can occur for $\beta=1$, corresponding to equal intensities of the pulses.

First we estimate W_{AS} for

$$(1-\Phi_0)\eta^2<1 , \tag{D21}$$

using the exact equation (D19). In the limit (D21),

$$\mathrm{erf}(ia)=\frac{-2i}{\sqrt{\pi}}(a+\tfrac{1}{3}a^3) ,$$

and, expanding $\exp(-b)$ up to the first order in the parameter $(1-\Phi_0)\eta^2$, one finds

$$\begin{aligned}A_\pm=\frac{4}{3\pi^2\sqrt{\pi}}\int_0^{\pi/2}d\phi_+\int_0^{\pi/2}d\phi_-\exp\left[-\frac{2\eta^2\sin^2\phi_-\sin^2\phi_+}{1\pm\sqrt{\Phi}\cos\phi_-\cos\phi_+}\right]\sin(2n\phi_-)\\ \times\left[\frac{\sqrt{2}G\eta\sin\phi_-\cos\phi_+}{\{(1\pm\sqrt{\Phi}\cos\phi_-\cos\phi_+)[1+D(1\pm\sqrt{\Phi}\cos\phi_-\cos\phi_+)]\}^{0.5}}\right.\\ +\frac{2\sqrt{2}G\eta^3\sin^3\phi_-\cos^3\phi_+}{\{(1\pm\sqrt{\Phi}\cos\phi_-\cos\phi_+)^3[1+D(1\pm\sqrt{\Phi}\cos\phi_-\cos\phi_+)]\}^{0.5}}\\ \left.\times\left[\frac{G^2}{3[1+D(1\pm\sqrt{\Phi}\cos\phi_-\cos\phi_+)]}-1+\Phi_0\right]\right] .\end{aligned} \tag{D22}$$

Taking into account the fact that the main contribution to the integral (D22) comes from the region $0\le\phi_+\ll1$, we first integrate Eq. (D22) over ϕ_+, putting $\sin\phi_+=\phi_+$ and $\cos\phi_+=1$ to obtain

$$\begin{aligned}A_\pm=\frac{2G}{3\pi^2}\int_0^{\pi/2}d\phi_-\frac{\sin(2n\phi_-)}{[1+D(1\pm\sqrt{\Phi}\cos\phi_-)]^{1/2}}\\ \times\left[1+\frac{2\eta^2\sin^2\phi_-}{1\pm\sqrt{\Phi}\cos\phi_0}\left[\frac{G^2}{3[1+D(1\pm\sqrt{\Phi}\cos\phi_0)]}-1+\Phi_0\right]\right] .\end{aligned} \tag{D23}$$

When $D\gg1$, $A_\pm\sim[\max(n,\sqrt{D})]^{-1}$ and leads to a negligibly small asymmetrical signal. Evaluating the integral (D23) under the assumption that $D\ll1$ and subtracting A_- from A_+, one obtains

$$W_{AS}=\frac{2nG}{3\pi^2(4n^2-1)}\left[-D+4\eta^2\left[1-\Phi_0-\frac{G^2}{3}\right]\right] ; \tag{D24}$$

for $(1-\Phi)\ll n^2/\eta^2$, one recovers Eq. (6.39).

To estimate W_{AS} when $(1-\Phi_0)\eta^2>1$, one can use Eq. (D20) and calculate only A_+, as $A_+ \gg A_-$. If

$$1 \ll (1-\Phi_0)\eta^2 \ll n^2 , \tag{D25}$$

then $y_+ = n/\eta \ll 1$, and for the integration range $y_+ \le \phi_+ \le \pi/2$ in Eq. (D20), it follows that $\chi \ll 1$, and $\sin^2\phi_+ \gg (1-\Phi_0)$. Consequently, A_+ takes the form

$$A_+ = \frac{1}{3\pi\eta^2\sqrt{\pi}} \int_{y_+}^{\pi/2} \frac{Gn\cos\phi_+}{\sin^3\phi_+\sqrt{2D+1}} d\phi_+$$

$$= \frac{G}{6\pi n\sqrt{\pi(2D+1)}} , \tag{D26}$$

which leads to Eq. (6.40) for $D \ll 1$.

If $(1-\Phi_0)\eta^2 \gg n^2$, then $y_+ = 0$; and $\chi < 1$ for $y_0 \le \phi_+$, where

$$y_0 = \frac{Gn}{\eta[(1-\Phi_0)(1+2D\Phi_0)]^{1/2}} \exp\left[-\frac{\eta^2(1-\Phi_0)[(1-\sqrt{\Phi})+D(1-\Phi_0)]}{n^2G^2} \right] \ll \left[\frac{1-\Phi_0}{\Phi_0} \right]^{1/2} . \tag{D27}$$

The main contribution to the integral (D20) comes from the region $\phi_+ < 1$. Then one finds

$$A_+ = \frac{1}{3\pi\eta\sqrt{2\pi}} \left[\int_0^{y_0} \left[\frac{2}{1-\Phi_0+\Phi_0\phi_+^2} \right]^{1/2} d\phi_+ \right.$$

$$\left. + \frac{2Gn}{\eta\sqrt{\pi}} \int_{y_0}^1 \frac{d\phi_+}{(1-\Phi_0+\Phi_0\phi_+^2)[D(1-\Phi_0)+(1-\sqrt{\Phi})+\phi_+^2(0.5+D\Phi_0)]^{1/2}} \right] , \tag{D28}$$

which can be integrated exactly. We present here the results in the most important cases. If $D>1$,

$$W_{AS} = A_+ = \frac{2Gn}{3\pi^2\eta^2(1-\Phi_0)\sqrt{2D}} , \tag{D29}$$

which is negligibly small. If $D \ll 1$, one arrives at

$$W_{AS} = \frac{1}{3\pi\eta\sqrt{\pi}} \left[\frac{y_0}{(1-\Phi_0)^{1/2}} + \frac{2Gn}{\eta\sqrt{\pi}(1-\Phi_0)} \ln\left[\frac{2(1-\Phi_0)^{1/2}}{y_0+[y_0^2+(1-\sqrt{\Phi})+2D(1-\Phi_0)]^{1/2}} \right] \right] ; \tag{D30}$$

for $\Phi=1$ Eq. (D30) reduces to Eq. (6.41).

b. Signals of higher order: $n \gg \eta \gg 1$. In this case to estimate the signal one can use Eq. (D9) to obtain W_{AS}, as the inequality (D8) is only violated for very small t_{12}, where the variation of the signal is negligible.

For pulses with very different intensities,

$$\alpha_{max} \gg \alpha_{min} \gg t_p^{-1} , \tag{D31}$$

one has

$$\beta \ll 1 . \tag{D32}$$

If β is so small, that

$$\beta\frac{n^2}{\eta^2} \ll 1 , \tag{D33}$$

the asymmetrical part of the signal is negligible. For its symmetrical part, W_S, the main contribution to the integral (7) is from the region defined by $(1-\Phi_0\cos^2\phi_+) \approx 1$, leading to the result

$$W_n^{(3)} = \frac{1}{3\eta\pi\sqrt{2\pi}} \int_0^{\pi} \exp\left[-\frac{n^2}{2\eta^2}(1+\Phi_0\cos^2\phi_+) \right] d\phi_+$$

$$= \frac{1}{3\eta\sqrt{2\pi}} \exp\left[-\frac{(2+\Phi_0)n^2}{4\eta^2} \right] I_0\left[\frac{\Phi_0 n^2}{4\eta^2} \right] , \tag{D34}$$

where I_0 is a modified Bessel function, which is Eq. (6.45).

If

$$\Phi_0 \gg \beta \gg \frac{\eta^2}{n^2} , \tag{D35}$$

the result (34) is still valid. However, if

$$1 \gg \beta \gg \Phi_0, \frac{\eta^2}{n^2} ,$$

the major contribution to the integrals (D7) and (D9), which can be used in this case, comes from the region $y=\pi-\phi_+ \ll 1$, and the PT-3 signal is given by

$$W_n^{(3)} = \frac{1}{3\eta\pi\sqrt{2\pi}} \left[1 - s \operatorname{erf} \left[\frac{n}{\eta\sqrt{2}} [D + (1-\Phi)]^{-1/2} \right] \right] \int_0^{\pi} \exp \left\{ -\frac{n^2}{2\eta^2} \left[1 - \beta \left[1 - \frac{y^2}{2} \right] \right] \right\} dy$$

$$= \frac{e^{-n^2(1-\beta)/2\eta^2}}{3\pi n\sqrt{2\beta}} \left[1 - s \operatorname{erf} \left[\frac{n}{\eta\sqrt{2}} [D + (1-\Phi)]^{-1/2} \right] \right] , \tag{D36}$$

where s is defined by Eq. (2.21).

The signal has a negative asymmetry ($A_- > A_+$), which can be large, when $D\eta^2/n^2 < 1$.

In the limiting case of equal pulse intensities, $\alpha_1=\alpha_2$ or $\beta=1$, the region $y=\pi-\phi_+ \ll 1$ provides the main contribution to the integrals (D7) and (D9) for any G. Then for $G=0$ one has

$$W_n^{(3)} = \frac{1}{3\eta\pi\sqrt{2\pi}} \int_0^{\pi} \exp \left[-\frac{n^2(1+y^2/4)}{4\eta^2} \right] dy$$

$$= \frac{\sqrt{2}}{3n\pi} e^{-n^2/4\eta^2} . \tag{D37}$$

For $(1-\Phi_0)n^2/\eta^2 > 1$, the signal is given by

$$W_n^{(3)} = \frac{1}{6\eta\pi\sqrt{\pi}} \int_0^{\min\{\pi,(\Phi_0^{-1}-1)^{1/2}\}} \frac{y}{(1-\Phi_0)^{1/2}} \exp \left[-\frac{n^2 y^2}{4\eta^2(1-\Phi_0)} \right] \times \left[1 - \operatorname{erf} \left[\frac{Gn}{\eta\{2(1-\Phi_0)[D(1-\Phi_0)+2]\}^{1/2}} \right] \right] dy$$

$$= \frac{\eta(1-\Phi_0)^{1/2}}{3n^2\pi\sqrt{\pi}} \left[1 - \operatorname{erf} \left[\frac{Gn}{\eta\{2(1-\Phi_0)[D(1-\Phi_0)+2]\}^{1/2}} \right] \right] ; \tag{D38}$$

for $\Phi=1$, Eq. (D38) reduces to Eq. (6.47).

[1] S. Asaka, H. Nakatsuka, M. Fujiwara, and M. Matsuoka, Phys. Rev. A **29**, 2286 (1984).

[2] H. Nakatsuka, M. Tomita, M. Fujiwara, and S. Asaka, Opt. Commun. **52**, 150 (1984).

[3] N. Morita and T. Yajima, Phys. Rev. A **30**, 2525 (1984).

[4] M. Fujiwara, R. Kuroda, and H. Nakatsuka, J. Opt. Soc. Am. B **2**, 1634 (1985).

[5] J. E. Golub and T. W. Mossberg, J. Opt. Soc. Am. B **3**, 554 (1986).

[6] J. E. Golub and T. W. Mossberg, Opt. Lett. **11**, 431 (1986).

[7] M. Tomita and M. Matsuoka, J. Opt. Soc. Am. B **3**, 560 (1986).

[8] M. Defour, J.-C. Keller, and J.-L. Le Gouët, J. Opt. Soc. Am. B **3**, 544 (1986).

[9] T. Hattori, A. Terazaki, and T. Kobayashi, Phys. Rev. A **35**, 715 (1987).

[10] K. Kurokawa, T. Hattori, and T. Kobayashi, Phys. Rev. A **36**, 1298 (1987).

[11] R. Beach, D. De Beer, and S. R. Hartmann, Phys. Rev. A **32**, 3467 (1985).

[12] M. Defour, J.-C. Keller, and J.-L. Le Gouët, Phys. Rev. A **36**, 5226 (1987).

[13] P. Tchénio, A. Debarre, J.-C. Keller, and J.-L. Le Gouët, Phys. Rev. A **38**, 5235 (1988).

[14] P. Tchénio, A. Debarre, J.-C. Keller, and J.-L. Le Gouët, Phys. Rev. A **39**, 1970 (1989).

[15] P. Tchénio, A. Debarre, J.-C. Keller, and J.-L. Le Gouët, Phys. Rev. Lett. **62**, 415 (1989).

[16] K. Wynne, M. Müller, and J. D. W. Van Voorst, Phys. Rev. Lett. **62**, 3031 (1989).

[17] X. Mi, H. T. Zhou, R. H. Zhang, and P. X. Ye, J. Opt. Soc. Am. B **6**, P184 (1989).

[18] J. Cooper, A. Charlton, D. R. Meacher, P. Ewart, and G. Alber, Phys. Rev. A **40**, 5705 (1989).

[19] For the references prior to 1984 see the reasonably complete list in B. W. Shore, J. Opt. Soc. Am. B **1**, 176 (1984).

[20] V. Finkelstein, Phys. Rev. A **27**, 961 (1984).

[21] S. N. Dixit and A. T. Georges, Phys. Rev. A **29**, 200 (1984).

[22] P. T. Greenland, J. Phys. B **17**, 1919 (1984).

[23] J. H. Eberly, K. Wodkiewicz, and B. W. Shore, Phys. Rev. A **30**, 2381 (1984).

[24] K. Wodkiewicz, B. W. Shore, and J. H. Eberly, Phys. Rev. A **30**, 2390 (1984).

[25] G. Hazak, M. Strauss, and J. Oreg, Phys. Rev. A **32**, 3475 (1985).

[26] I. Schek and J. Jortner, Chem. Phys. **97**, 1 (1985).

[27] Y. Prior, I. Schek, and J. Jortner, Phys. Rev. A **31**, 3775

(1985).
[28]S. Swain, J. Opt. Soc. Am. B **2**, 1666 (1985).
[29]K. Wodkiewicz and J. H. Eberly, J. Opt. Soc. Am. B **3**, 628 (1986).
[30]F. Rohart, J. Opt. Soc. Am. B **3**, 622 (1986).
[31]P. Franken and C. H. Joachain, Phys. Rev. A **36**, 1663 (1987).
[32]R. Boscaino and R. N. Mantegna, Phys. Rev. A **36**, 5482 (1987).
[33]M. W. Hamilton, K. Arnett, S. J. Smith, D. S. Elliot, M. Dziemballa, and P. Zoller, Phys. Rev. A **36**, 178 (1987).
[34]V. Finkelstein and V. Namiot, Moscow Univ. Phys. Bull. **42**, 81 (1987).
[35]G. S. Agarwal, C. V. Kunasz, and J. Copper, Phys. Rev. A **36**, 143 (1987).
[36]B. H. W. Hendriks and G. Nienhuis, Phys. Rev. A **36**, 5615 (1987).
[37]T. A. B. Kennedy and S. Swain, Phys. Rev. A **36**, 1747 (1987).
[38]Th. Haslwanter, H. Ritsch, J. Cooper, and P. Zoller, Phys. Rev. A **38**, 5652 (1988).
[39]A. I. Burshtein, A. A. Zharikov, and S. I. Temkin, J. Phys. B **21**, 1907 (1988).
[40]A. G. Kofman, R. Zaibel, A. M. Levine, and Y. Prior, Phys. Rev. Lett. **61**, 251 (1988).
[41]R. G. Friedberg and S. R. Hartmann, J. Phys. B **21**, 683 (1988).
[42]W. G. Van Kampen, *Stochastic Processes in Physics and Chemistry* (North-Holland, Amsterdam, 1981), Chap. XIV.
[43]*Handbook of Mathematical Functions,* edited by M. Abramowitz and I. A. Stegun (Dover, New York, 1980).
[44]V. Finkelstein, Zh. Eksp. Teor. Fiz. **78**, 2138 (1980) [Sov. Phys.—JETP **51**, 1072 (1980)].